REPORT 1142

DIFFUSION OF HEAT FROM A LINE SOURCE IN ISOTROPIC TURBULENCE[1]

By MAHINDER S. UBEROI and STANLEY CORRSIN

SUMMARY

An experimental and analytical study has been made of some features of the turbulent heat diffusion behind a line heated wire stretched perpendicular to a flowing isotropic turbulence. The mean temperature distributions have been measured with systematic variations in wind speed, size of turbulence-producing grid, and downstream location of heat source. The nature of the temperature fluctuation field has been studied.

A comparison of Lagrangian and Eulerian analyses for diffusion in a nondecaying turbulence yields an expression for turbulent-heat-transfer coefficient in terms of turbulence velocity and a Lagrangian "scale."

The ratio of Eulerian to Lagrangian microscale has been determined theoretically by generalization of a result of Heisenberg and, with arbitrary constants taken from independent sources, shows rough agreement with experimental results.

A convenient form has been deduced for the criterion of interchangeability of instantaneous space and time derivatives in a flowing turbulence.

INTRODUCTION

One of the most striking aspects of turbulent motion in fluids is its dispersive property. This "convective diffusion," illustrated by the general statistical tendency of (noncontiguous) fluid elements to get farther apart with increasing time, was probably first observed long before the era of analytical fluid mechanics. An analytical start on this problem was not made, however, until the now-classic work by Taylor in 1921 on diffusion by continuous movements (reference 1). Not only did this paper lay a groundwork for the study of turbulent diffusion but it also represented a forward step in the ideas essential to development of a general statistical theory of turbulence, a field which had scarcely progressed since Reynolds' original formulation of the equations of motion for a flow in which mean and fluctuating parts could be distinguished.

The diffusive action of a turbulent flow may manifest itself in various ways, depending upon the initial and/or boundary conditions and upon the interests of the observer. The following possible measures of the diffusive powers are neither exhaustive nor mutually independent:

(1) The average rate of dispersion of particles from a fixed source
(2) The average rate of increase of spacing between different particles
(3) The average rate of transport of particle concentration under a given mean concentration gradient
(4) The average rate of increase of the length of a fluid line
(5) The average rate of increase of the area of a fluid surface

The word "particles" means simply indelibly tagged fluid elements, much smaller than the smallest length associated with the turbulence.

The present report is concerned primarily with measure (1). The measurements have all been made in the thermal wake of a long thin heated wire mounted perpendicular to an isotropic turbulent air flow and producing no turbulent wake. Here the tagging is thermal, and the degree of indelibility (negligibility of molecular diffusion) is one of the matters to be investigated.

The diffusive property (for scalars) of a turbulent flow is apparently a secondary characteristic at least in the sense that it need not explicitly enter the dynamical problem. The diffusion may be regarded as a kinematic phenomenon, to be deduced from the dynamical solution to the problem if and when the latter is obtained. Thus the objective of research on turbulent diffusion may be to seek a connection between the diffusive and the dynamical statistical variables, even before the complete dynamical theory is available.

Measure (3) is usually termed the "turbulent transport" or "transfer" problem. Although of extensive practical importance, it has not yet been subjected to genuine theoretical study.

Most of the semiempirical "theories" of turbulent transport, for both scalar and vector properties, employ an Eulerian formulation of the basic equations, and up to now they have been unable to relate the turbulent transport correlation to other statistical functions describing the flow. Taylor (reference 1) showed that in the simple case of a homogeneous field of isotropic turbulence, and even in a decaying isotropic turbulence (reference 2), a Lagrangian formulation of the transport (i. e., diffusion; the terms will be used interchangeably) problem leads to some important results.[2]

Up to the present time little theoretical or experimental work has been done to find relations, if any, between the Lagrangian statistical measures of a turbulent field with its Eulerian statistical measures. Since turbulence dynamics seems best handled in the latter terms and turbulent diffusion in the former, it is evident that such a connection is impor-

[1] Supersedes NACA TN 2710, "Diffusion of Heat From a Line Source in Isotropic Turbulence" by Mahinder S. Uberoi and Stanley Corrsin, 1952.

[2] In his tensorial generalization of Taylor's work on case (1), Batchelor (reference 3) has chosen to call this an "Eulerian" analysis, describing only case (2) as "Lagrangian." In keeping with previously accepted nomenclature, both cases are Lagrangian, (1) involving a single particle and (2) involving a pair. In fact, case (2) might be termed a mixed (Eulerian and Lagrangian) problem.

tant. Hence, one of the purposes of the present experiments has been to compare the magnitudes of some of these quantities under variations in the turbulent field. For example, the postulates of Taylor and Heisenberg on a relation between Lagrangian and Eulerian microscales can be examined and, in corrected form, compared with experiment.

The turbulent diffusion from a fixed line source can be set up analytically as an ordinary (Eulerian) "heat-transfer" problem, permitting a start to be made in relating measures (1) and (3) of the diffusive power of a turbulent flow, under certain simplifying assumptions.

Measures (4) and (especially) (5) may well be classed as characteristic of the "turbulent-mixing" problem rather than diffusion in the common connotation.

Experimental work on diffusion from a fixed local source in a turbulent flow has been meager. In isotropic turbulence, there have been the measurements of Schubauer (reference 4), Simmons (reported by Taylor in reference 2), Dupuis (reported by Kampé de Feriet in reference 5), Frenkiel (reference 6), and Collis (reference 7). Of these, only the data of Simmons and Collis are extensive enough to permit confident computation of the Lagrangian correlation function. In turbulent shear flow, Skramstad and Schubauer (reference 8), Dryden (reference 9), and the present authors (reference 10) have measured distributions close to a source; Kalinske and Pien (reference 11) and Van Driest (reference 12) have made measurements somewhat farther downstream.

None of these studies was repeated with a systematic variation of the properties of the turbulence. In spite of the poor precision inherent in this type of measurement, it was hoped that such an approach would at least show up some general trends in the relations between Eulerian and Lagrangian variables.

This investigation has been conducted at the Aeronautics Department of the Johns Hopkins University under the sponsorship and with the financial assistance of the National Advisory Committee for Aeronautics. The authors would like to acknowledge the assistance of Messrs. Alan Kistler, George Stierhoff, and Allen Gates and Miss Patricia O'Brien, as well as the helpful criticism of Dr. Francis H. Clauser and Dr. C. C. Lin.

SYMBOLS

c root-mean-square molecular velocity

c_p specific heat per unit volume at constant pressure

$f(r)$ Eulerian velocity correlation coefficient (notation of Von Kármán and Howarth)

$H \equiv 2\rho c_p \overline{U} \int_0^\infty \overline{\Theta}\, dy$

$H^* \equiv \dfrac{H}{2\rho c_p \int_0^\infty f(\xi) d\xi}$

j width of rectangular heat pulse

k thermal conductivity

k_T turbulent-heat-transfer coefficient

L Eulerian scale $\left(L \equiv \int_0^\infty f(r) dr\right)$

L_L Lagrangian scale $\left(L_L \equiv \int_0^\infty R_\tau(\tau) d\tau\right)$

L_η Lagrangian scale for nondecaying and decaying turbulence $\left(L_\eta \equiv \int_0^\infty R_\eta(\eta) d\eta\right)$

l mixing length

M grid mesh size

$M_1 \equiv \int_0^\infty \eta R_\eta(\eta) d\eta$

$P(\vartheta)$ probability density of fluctuating temperature

p static pressure

R_L turbulence Reynolds number based on Eulerian scale $\left(R_L \equiv \dfrac{u'L}{\nu}\right)$

$R_{t-\tau} \equiv R_\tau(t, \tau) \equiv \dfrac{\overline{v(t)v(t-\tau)}}{v'(t)v'(t-\tau)}$

$R_\tau(\tau)$ Lagrangian correlation coefficient for nondecaying turbulence

$R_\eta(\eta)$ Lagrangian correlation as a function of η for nondecaying and decaying turbulence

$R_{\vartheta v} \equiv \dfrac{\overline{\vartheta v}}{\overline{\Theta U}}$

R_λ turbulence Reynolds number based on Eulerian microscale $\left(R_\lambda \equiv \dfrac{v'\lambda}{\nu}\right)$

r scalar distance between two points

$S \equiv -\overline{\left(\dfrac{\partial v}{\partial y}\right)^3} \Big/ \left[\overline{\left(\dfrac{\partial v}{\partial y}\right)^2}\right]^{3/2}$

s average on-center spacing of pulses

$T \equiv \left[\overline{\left(\dfrac{dv}{dt}\right)^2} \Big/ \overline{U}^2 \overline{\left(\dfrac{\partial v}{\partial x}\right)^2}\right]^{1/2}$

t time

$\overline{U}$ mean velocity in x-direction

u instantaneous velocity fluctuation in x-direction

$u' \equiv \sqrt{\overline{u^2}}$

$\overline{V}$ mean velocity in y-direction

v instantaneous velocity fluctuation in y-direction

$v' \equiv \sqrt{\overline{v^2}}$

w instantaneous velocity fluctuation in z-direction

X distance traveled in x-direction by a fluid particle

x distance downstream from grid

x_o location of heating wire

$\Delta x = x - x_o$

Y distance traveled in y-direction by a fluid particle

Y' root-mean-square displacement of a fluid particle in y-direction $\left(Y' \equiv \sqrt{\overline{Y^2}}\right)$

Y_m root-mean-square displacement of a molecule

y distance in direction of measured diffusion

z distance in direction of heating wire

$\epsilon \equiv \dfrac{\partial v}{\partial t} + U \dfrac{\partial v}{\partial x}$

$\eta(t_o,t)\equiv\int_{t_o}^{t}v'(\xi)d\xi$

Θ instantaneous temperature (measured above ambient room temperature)

$\overline{\Theta}$ mean temperature

$\overline{\Theta}_o$ maximum mean temperature at a cross section, a function of Δx

ϑ instantaneous temperature difference

$\vartheta'\equiv\sqrt{\overline{\vartheta^2}}$

ϑ_o temperature difference of rectangular heat pulse

κ dimensionless empirical constant

Λ mean free path of a molecule

λ Eulerian microscale of turbulence $\left(\lambda\equiv\left(\frac{1}{-f''(0)}\right)^{1/2}\right)$

λ_r Lagrangian microscale of turbulence for nondecaying turbulence $\left(\lambda_r\equiv\left(\frac{2}{-R_r''(0)}\right)^{1/2}\right)$

λ_η Lagrangian microscale of turbulence for nondecaying and decaying turbulence $\left(\lambda_\eta\equiv\left(\frac{2}{-R_\eta''(0)}\right)^{1/2}\right)$

ν kinematic viscosity

$\xi\equiv\frac{y}{Y'(x)}$

ρ density

τ time difference

$(^-)$ mean value or ensemble average

Subscripts:

max maximum

min minimum

EQUIPMENT AND PROCEDURE

AERODYNAMIC EQUIPMENT

The wind tunnel (fig. 1) is an open-return NPL type tunnel with a 2- by 2-foot working section and a free-stream turbulence level of $v'/\overline{U}=0.06$ percent and $u'/\overline{U}=0.05$ percent at a mean velocity of 26 feet per second. The turbulence-producing grids were as follows:

Designation	Type	Mesh size (in.)	Rod diameter (in.)	Solidity
1-in. grid	Biplane, wood	1.00	0.25	0.437
½-in. grid	Woven, metal	*.50 by 0.53	.120	.41
¼-in. grid	Woven, metal	.25	.060	.42

* The 0.50-in. mesh was set in direction of measured diffusion.

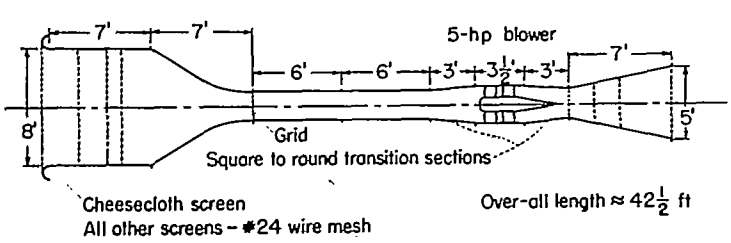

FIGURE 1.—Sketch of open-return wind tunnel.

321695—55——52

They were mounted in turn at the upstream end of the working section.

The heat source was an 0.008-inch-diameter platinum wire stretched vertically across the tunnel at various distances from the grid. It was heated by direct current to temperatures between 500° and 700° C, with the latter figure only at the highest operating velocity of 38.0 feet per second. The wire Reynolds numbers at this condition and at the two other velocities were as follows:

Mean speed (fps)	Wire temperature (°C)	Reynolds number based on—	
		Air temperature	Wire temperature
8.5	500	35	6 4
25.6	500	105	19
38.0	700	157	19

A preliminary investigation was made without grids to insure that these operating conditions did not generate a vortex street downstream of the heated wire.

With the grids in place, the mean momentum wake became practically undetectable with total-head tube and manometer at distances greater than 1 or 2 inches downstream of the heating wire.

MEASURING EQUIPMENT AND PROCEDURES

The mean-temperature distributions were measured with a Chromel-Alumel thermocouple and a Leeds and Northrup type K–2 potentiometer. The cold junction was kept outside of the wind tunnel.

The shadowgraph technique was used to photograph the laminar thermal wake close to the source with no grid in the wind tunnel. This information was applied to the problem of "correcting" the thermal wake in turbulent flow for the effects of molecular diffusion and of finite source size. Figure 2 (a) is a shadowgraph of the wire wake with no grid in the tunnel; figure 2 (b) is a typical time exposure with grid-produced turbulence. A resistance-thermometer traverse of the laminar wake in a flow of very small turbulence showed that the temperature profile had already become very nearly Gaussian at a distance of 1 inch (125 wire diameters) downstream. The white lines on the sides of the dark wake shadow in figure 2 (a) correspond to the minimums in the second derivative of the density profile. For small temperature differences these coincide with the maximums in the second derivative of the temperature profile. Although the temperature differences are not small in the immediate vicinity of the wire, this condition is reasonably well satisfied at relatively small values of Δx as evidenced by the parabolic spread of this laminar wake.

The standard deviation of the wake could then be computed from the spacing of these two bright lines, with the assumption of a Gaussian distribution. Since the closest points of traverse in the turbulent cases were ½ inch (63 wire diameters) from the heat source, this was probably a reasonable assumption.

As pointed out by Taylor (reference 2), the molecular and

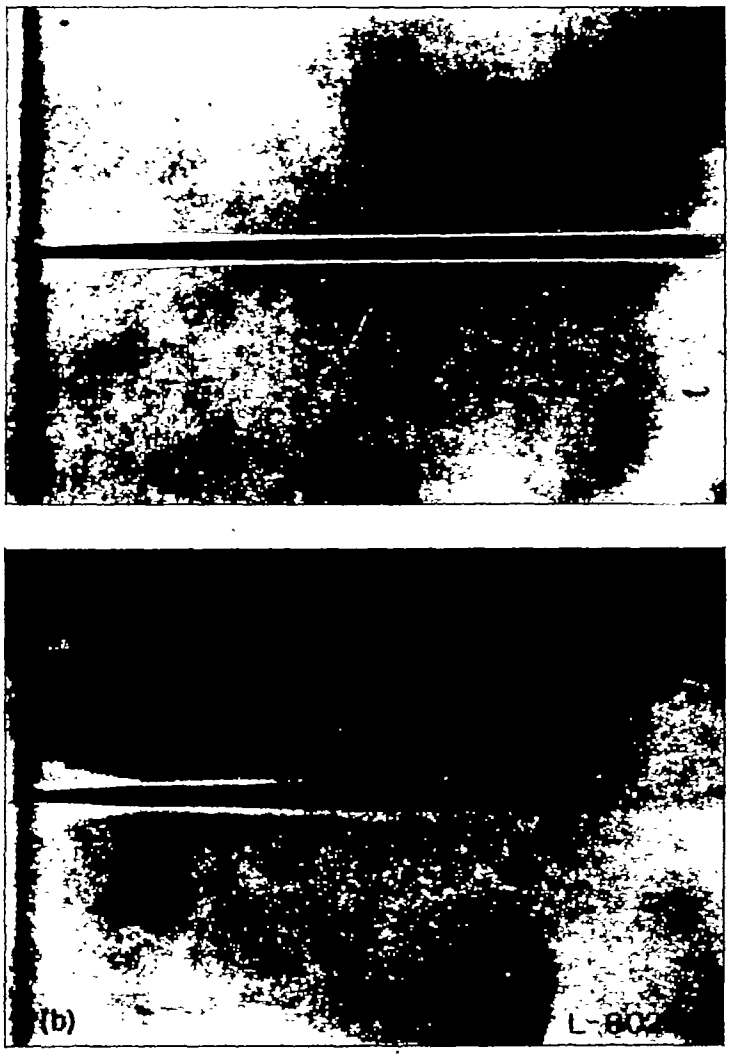

(a) No grid in tunnel.
(b) Grid-produced turbulence.

FIGURE 2.—Shadowgraph time exposure of wire wake.

the turbulent diffusive phenomena are statistically independent, so that the squares of the standard deviations due to these two effects are additive. Hence the wake spread due to turbulence alone, from a true line source, was obtained by subtracting the square of the standard deviation of the laminar wake (computed from the shadowgraph) from the square of the standard deviation of the total wake (from thermocouple traverses with grid turbulence present) at all stations. This difference was the square of the standard deviation of the desired phenomena. All wake-spread data presented in the next section have been corrected in this fashion.

Parenthetically, it should be remarked that the laminar wake in figure 2 (a) spreads parabolically within the limits of precision, from at least 1 inch on, so that the effects of density differences on the flow phenomena must have been negligible for this investigation.

The transverse turbulence levels $v'/\overline{u}$ behind the grids were obtained from the initial rate of spread of the mean thermal wake (method due to Schubauer (reference 4)) after the effects of molecular spread and finite source had been removed. The resulting levels were somewhat higher than those obtained with a hot-wire anemometer but were used because of their consistency with the rest of the measured diffusion curve.

Free-stream velocity fluctuations (without grids) and the wake temperature fluctuations (with grids) were measured with the hot-wire anemometry equipment described in reference 10. The wires were 0.00025-inch platinum etched from Wollaston; the compensated response of the system was flat within ± 2 percent over a frequency range from 3 to 12,000 cycles per second.

Oscillograms of the temperature fluctuations were recorded by photographing a blue oscilloscope tube with fast 35-millimeter film in a General Radio type 651–AE camera.

Probability densities of the temperature fluctuations at fixed points in the mean thermal wake were determined from photodensitometer traverses of time-exposure photographs of a short-persistence (0.001 sec) blue oscilloscope tube with the temperature fluctuations on one pair of plates and a 30,000-cycle-per-second sweep on the opposite plates. The technique is essentially that used by Simmons and Salter (reference 13).

EXPERIMENTAL RESULTS

MEAN THERMAL WAKE.

Complete mean-temperature wakes behind a line source of heat were measured for 10 different conditions. Arranged to indicate the systematic variation of one parameter at a time, these conditions were as follows:

1-in. grid; $\frac{x_o}{M}$=43.4; $\overline{U}$, fps	8.5 25.6 38.0
$\overline{U}$=25.6 fps; $\frac{x_o}{M}$=43.4; grid, in	1 ½ ¼
$\overline{U}$=25.6 fps; $\frac{x_o}{M}$=86.1; grid, in	1 ½ ¼
$\overline{U}$=25.6 fps; ½-in. grid; x_o/M	43.4 86.1 172.3
$\overline{U}$=25.6 fps; ¼-in. grid; x_o/M	43.4 86.1 172.3

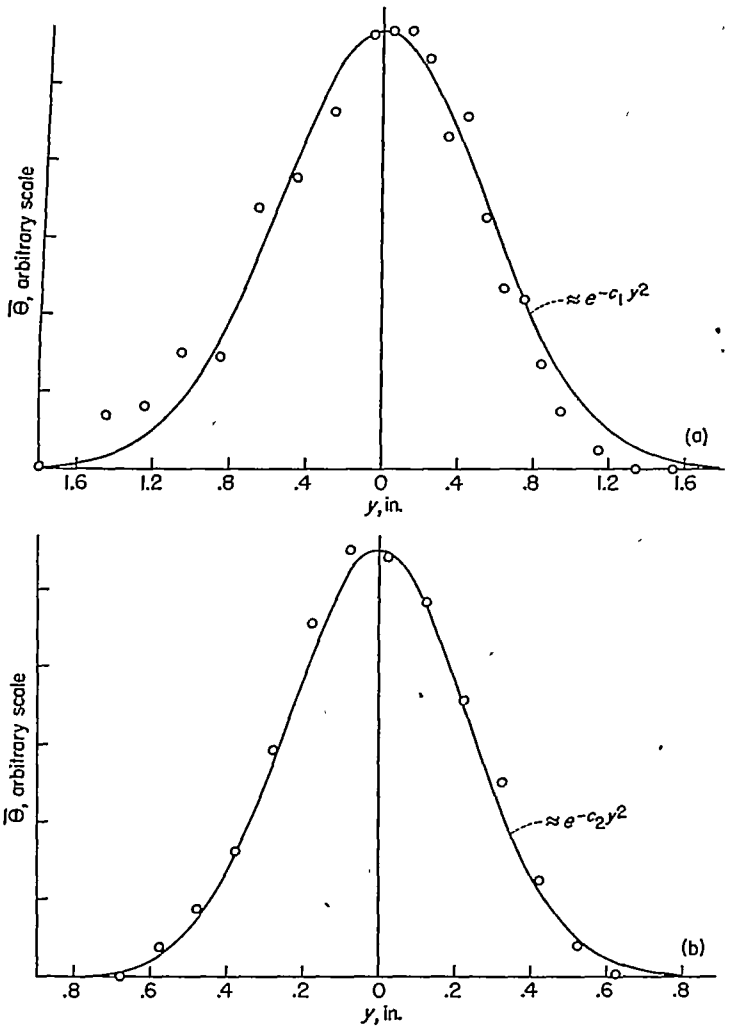

(a) $\frac{\Delta x}{M}=15$, $\frac{x_o}{M}=43.4$, $M=1$ inch, and $\overline{U}=25.6$ feet per second.

(b) $\frac{\Delta x}{M}=39$, $\frac{x_o}{M}=86.1$, $M=\frac{1}{4}$ inch, and $\overline{U}=25.6$ feet per second.

FIGURE 3.—Experimental scatter; temperature behind line source of heat.

Here $\overline{U}$ is the mean velocity, M is the grid mesh size, and x_o is the heat-source location measured from the grid. Since some individual cases enter as elements in two sequences, the total number of elements is more than 10.

Two of the many mean-temperature traverses in the y-direction (perpendicular to mean flow and to source line) are shown in figure 3 to give an idea of the amount of experimental scatter. The upper traverse was the worst of the lot, even showing an apparent skewness which was not borne out by the investigation as a whole. The lower traverse is more nearly typical of the measured temperature distributions from which the standard deviations of the mean

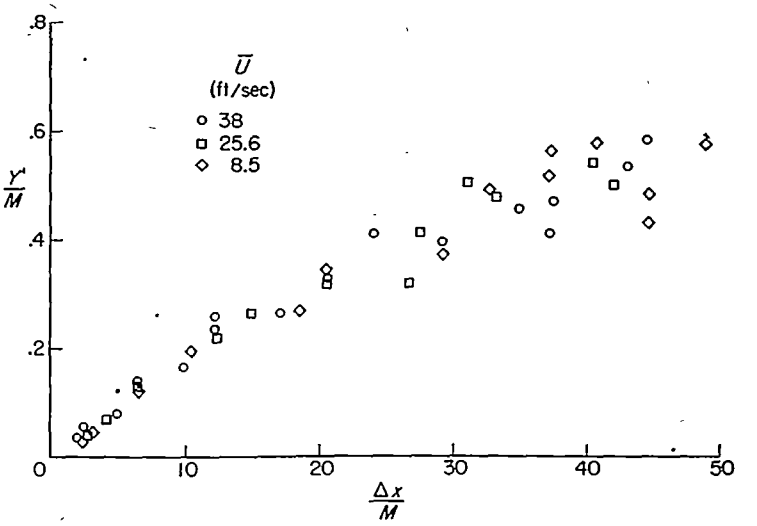

FIGURE 4.—Spread of heat from a line source. $\frac{x_o}{M}=43.4$, $M=1$ inch.

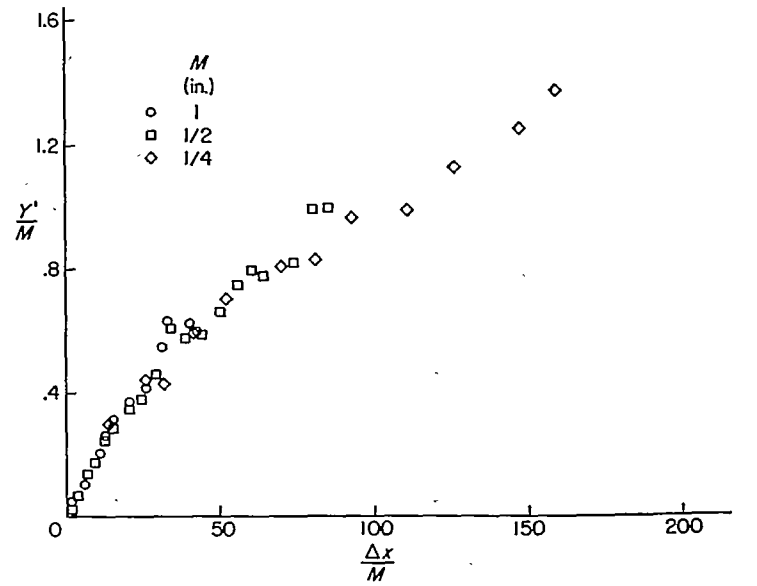

FIGURE 5.—Spread of heat from a line source. $\frac{x_o}{M}=43.4$, $\overline{U}=25.6$ feet per second.

thermal wake were computed. By comparison with the reference curve, it is seen to be essentially Gaussian. This was the case for temperature profiles at all stations. Since the virtually Gaussian character of such a wake has already been established by several of the earlier publications, there seemed to be no point in reproducing here all of the large number of traverses measured.

The mean-thermal-wake spread for the 10 different configurations studied is given in figures 4 to 7 as plots of corrected standard deviation Y' against distance from the heat

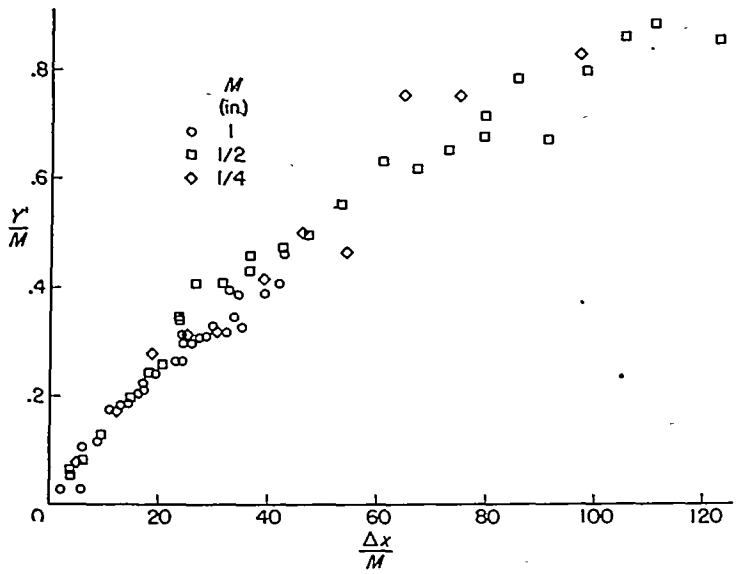

FIGURE 6.—Spread of heat from a line source. $\frac{x_o}{M}$=86.1, $\overline{U}$=25.6 feet per second.

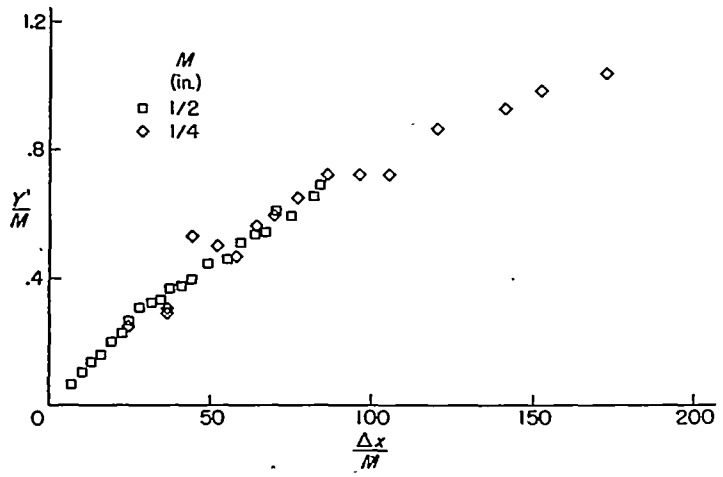

FIGURE 7.—Spread of heat from a line source. $\frac{x_o}{M}$=172.25, $\overline{U}$=25.6 feet per second.

source Δx. Each point in these figures corresponds to a complete transverse temperature traverse.

In order to have values of transverse turbulence level $v'/\overline{U}$ consistent with the thermal-wake behavior, these values were determined from the initial angle of spread of the corrected wake standard deviation (references 2 and 4) instead of from direct hot-wire anemometer measurements. The results are plotted in figure 8. Since these represent an insufficient number of points per grid to permit the drawing of reliable curves, some simplifying assumptions were made based upon the results of several more-detailed turbulence-decay investigations. (See references 14 to 20. The pertinent results of references 14 to 16 are summarized in reference 17.) In the light of these papers, it was assumed that the decay curves had a common apparent origin and that this was obtainable by drawing the best straight line for all the available points, independent of the differing wind speeds and mesh sizes. In computing any individual Lagrangian correlation function from the corresponding wake history, the turbulence decay rate was assumed to be given by the line drawn through this common origin and the specific turbulence value giving the measured initial spread angle for this wake. This is, of course, a very rough procedure, but the experimental scatter in this whole method of determining Lagrangian correlation functions is so great that a more extensive study of decay (including the resolution of inconsistencies between wake method and hot-wire method) seemed unwarranted at this time.

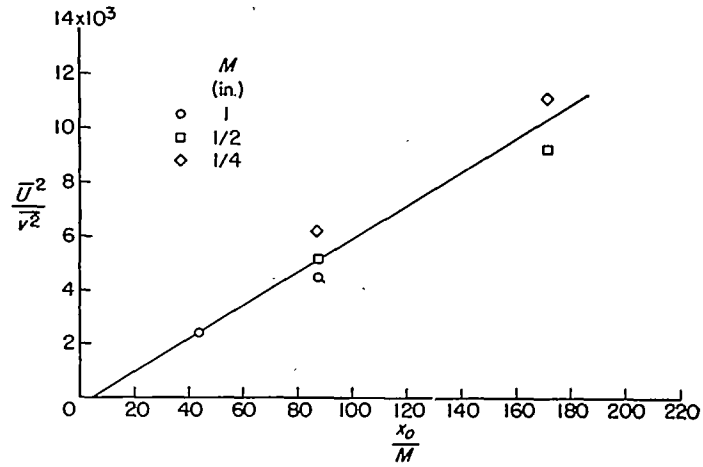

M (in.)	x_o/M	$\overline{U}$ (fps)	$v'/\overline{U}$ (percent)
1	43.4	8.5	2.0
1	43.4	25.6	2.0
1	43.4	38.0	2.0
1/2	43.4	25.6	2.0
1/4	43.4	25.6	2.0
1	86.1	25.6	1.50
1/2	86.1	25.6	1.40
1/4	86.1	25.6	1.30
1/2	172.3	25.6	1.05
1/4	172.3	25.6	.95

FIGURE 8.—Decay of turbulence as determined by thermal wake of a line source.

TEMPERATURE FLUCTUATIONS

Distributions of temperature-fluctuation level $\vartheta'/\overline{\Theta}$ in the thermal wake have been measured by using the hot-wire anemometer as a resistance thermometer, that is, at a current low enough to render the sensitivity to velocity fluctuations negligible compared with the sensitivity to temperature fluctuations (reference 21). A representative distribution of $\vartheta'/\overline{\Theta}$ in the x-direction is given in figure 9. Typical transverse distributions are given in figures 10 (a) and 10 (b). It is clear that the temperature-fluctuation inten-

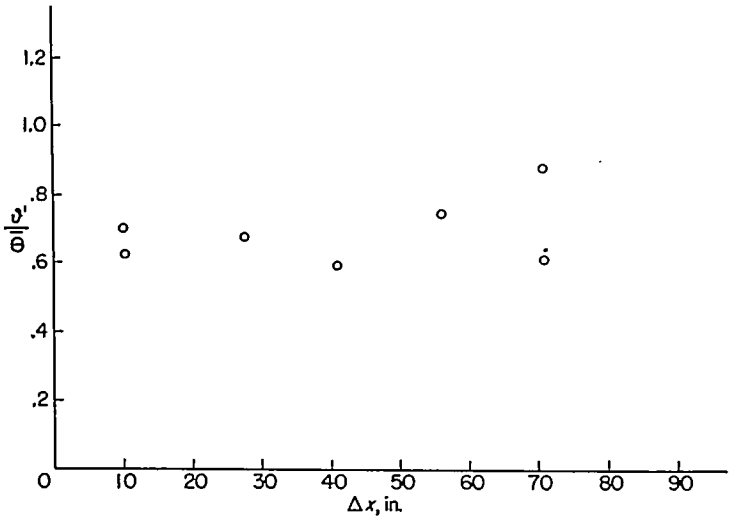

FIGURE 9.—Temperature fluctuations at $x_o=43$ inches, $M=1$ inch, and $\overline{U}=25.6$ feet per second along wake axis.

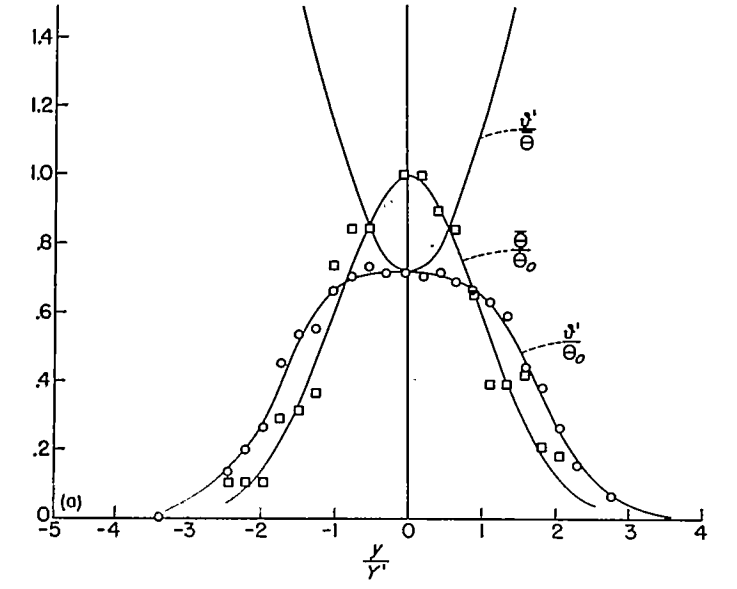

(a) $\Delta x=10$ inches.

FIGURE 10.—Temperature fluctuations behind a line heat source at $\frac{x_o}{M}=43$, $M=1$ inch, and $\overline{U}=25.6$ feet per second.

sity changes very little with increasing values of Δx. A rough explanation of the very high values of ϑ'/Θ (compared with the concomitant turbulence level, for example) in terms of the highly intermittent structure of the thermal wake has been given in reference 10 and will be discussed in more detail later in this report. This intermittency is shown very clearly in figure 11, a series of temperature oscillograms recorded at two different positions across the thermal wake for a fixed value of Δx and at two different

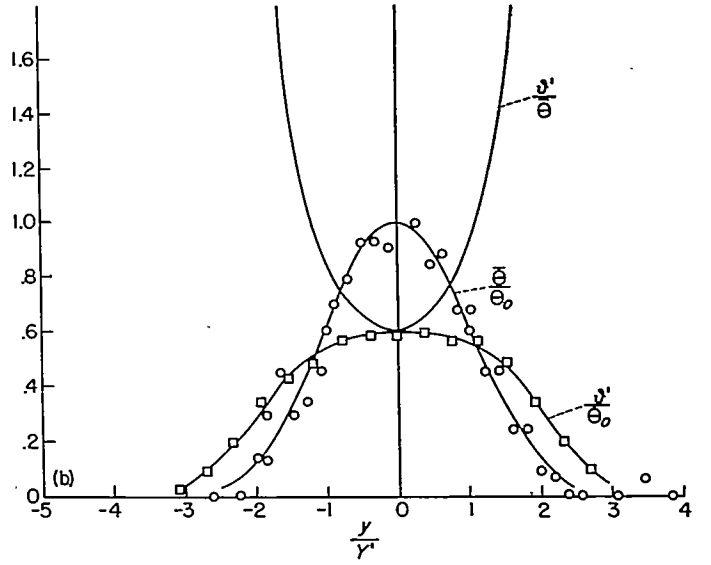

(b) $\Delta x=70$ inches.

FIGURE 10.—Concluded.

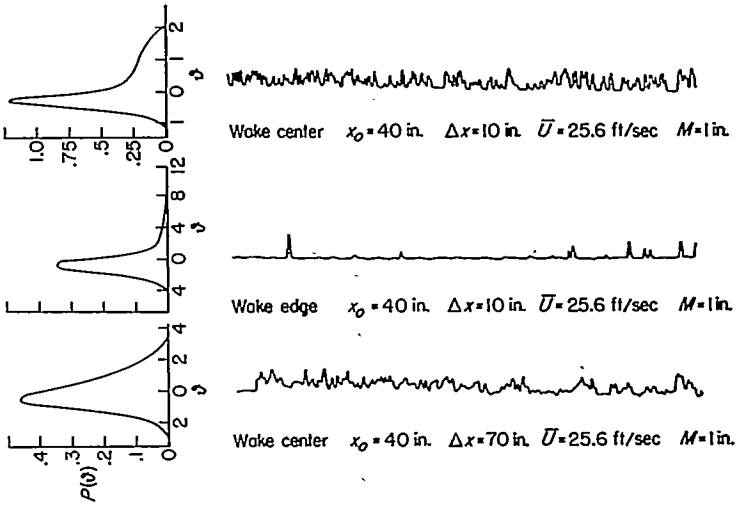

FIGURE 11.—Oscillogram records and normalized probability density of temperature fluctuations. Film speed, 1 foot per second.

values of Δx with $y=0$. The one-sided and pulse character of the instantaneous temperature at a fixed point in space is also demonstrated by its probability density.

THEORETICAL CONSIDERATIONS

HOMOGENEOUS STEADY TURBULENCE AT REST

For a nondecaying incompressible turbulence with no mean motion, Taylor (reference 1) was followed in getting an expression for the mean time rate of diffusion in the y-direction (say) from a fixed source as measured by the second moment of the probability density of the diffusion, that is, the mean-square particle displacement $\overline{Y^2(t)}$:

$$\frac{d}{dt}\overline{Y^2}=2\overline{Y\frac{dY}{dt}}$$

$$=2\overline{v(t)\int_0^t v(t_1)dt_1}$$

The bar denotes ensemble average.

Taking $v(t)$ inside the integral, interchanging the processes of integration and averaging, and introducing the Lagrangian (auto) correlation coefficient (following the fluid particle), where $\tau=t-t_1$,

$$R_v(\tau)\equiv\frac{\overline{v(t)\,v(t-\tau)}}{\overline{v^2}}$$

there results

$$\overline{Y^2}=2\overline{v^2}\int_0^t\int_0^T R_v(\tau)d\tau dT \tag{1}$$

This is Taylor's form. Integration by parts yields a form like that in the work of Kampé de Feriet (reference 5):

$$\overline{Y^2}=2\overline{v^2}\int_0^t(t-\tau)R_v(\tau)d\tau \tag{2}$$

In this Lagrangian analysis, $v(t)$ is the velocity of a fluid particle in the y-direction at time t; $v(t-\tau)$ is the velocity of the same particle at time $t-\tau$. Corresponding expressions can be written for the rate of diffusion in any direction.

Diffusion from an infinite line source, the case to be discussed here, is a two-dimensional problem in the mean, and, in addition to equation (2),

$$\overline{X^2}=2\overline{u^2}\int_0^t(t-\tau)R_u(\tau)d\tau \tag{3}$$

A tensorial generalization of these concepts has been given by Batchelor (reference 3) dealing with the behavior of $\overline{X_iX_j}(t)$ where X_i and X_j are any two of the orthogonal displacements of the particle at time t.

It should be noted that this analysis gives no information on the shape of the probability density of $Y(t)$ or of $X(t)$. In fact there still exists no theory for these. However, experiments in flowing turbulence (the case to be considered next) show Gaussian density, within the experimental precision, for $Y(t)$ at all values of t.

For this stationary random process, Taylor (reference 1) introduced the concept of the Lagrangian "scale,"

$$L_L=\int_0^\infty R_v(\tau)d\tau \tag{4}$$

These have the dimensions of time and are characteristic constants of the system.

In his later work on the (Eulerian) dynamics (reference 2), Taylor had occasion to introduce another measure of the correlation function, which he called the "microscale." Applying the same geometrical concept to the present function, the Lagrangian microscale

$$\lambda_v^2=-\frac{2}{R_v''(0)} \tag{5}$$

is simply the τ-intercept of the vertex-osculating parabola of the even function $R_v(\tau)$. The kinematic significance is clearly shown by a series expansion of $v(t+\tau)$ in $R_v(\tau)$:

$$R_v(\tau)=\frac{\overline{v(t)v(t+\tau)}}{\overline{v^2}}$$

$$=\frac{1}{\overline{v^2}}\left(\overline{v(t)\left\{v(t)+\left[\left(\frac{dv}{dt}\right)_t\right]\tau+\left[\left(\frac{d^2v}{dt^2}\right)_t\right]\frac{\tau^2}{2}+\cdots\right\}}\right)$$

$$=\frac{1}{\overline{v^2}}+\left\{\overline{v^2}\left[\frac{1}{2}\left(\frac{d\overline{v^2}}{dt}\right)_t\right]\tau+\left[\frac{1}{2}\left(\frac{d^2\overline{v^2}}{dt^2}\right)_t-\overline{\left(\frac{dv}{dt}\right)_t^2}\right]\frac{\tau^2}{2}+\cdots\right\}$$

But $\overline{v^2}=$Constant, so that

$$R_v(\tau)=1-\frac{1}{2\overline{v^2}}\overline{\left(\frac{dv}{dt}\right)^2}\tau^2+\cdots \tag{6}$$

From equations (6) and (5), the Lagrangian microscale for $v(t)$ is

$$\lambda_v^2=\frac{2\overline{v^2}}{\overline{\left(\frac{dv}{dt}\right)^2}} \tag{7}$$

or

$$\overline{\left(\frac{dv}{dt}\right)^2}=2\frac{\overline{v^2}}{\lambda_v^2} \tag{7a}$$

TURBULENCE IN A FLOWING MEDIUM

The dictates of both practical interest and experimental feasibility require analysis of the diffusion when there is a mean velocity $\overline{U}$ relative to the source. Since the diffusion phenomenon is linear, the probability density (mean-concentration distribution of tagged particles in the wake) is simply proportional to the superimposed probability densities of a continuous line of sources moving with the mean velocity $\overline{U}$ with their time (and space) origin at the actual fixed source. This is illustrated in figure 12(a) for $\frac{\overline{v'^2}}{\overline{U}}<1$. The circles (corresponding to isotropy) are the standard deviations of the dispersions that would occur from moving sources. The envelope of these circles gives a measure of the mean wake. It is obvious that in general the functional form of the mean-concentration distribution along a line $\Delta x=$Constant will not be the same as the functional form of the same quantity for the individual source at time t, that is, at position $x=\overline{U}t$.

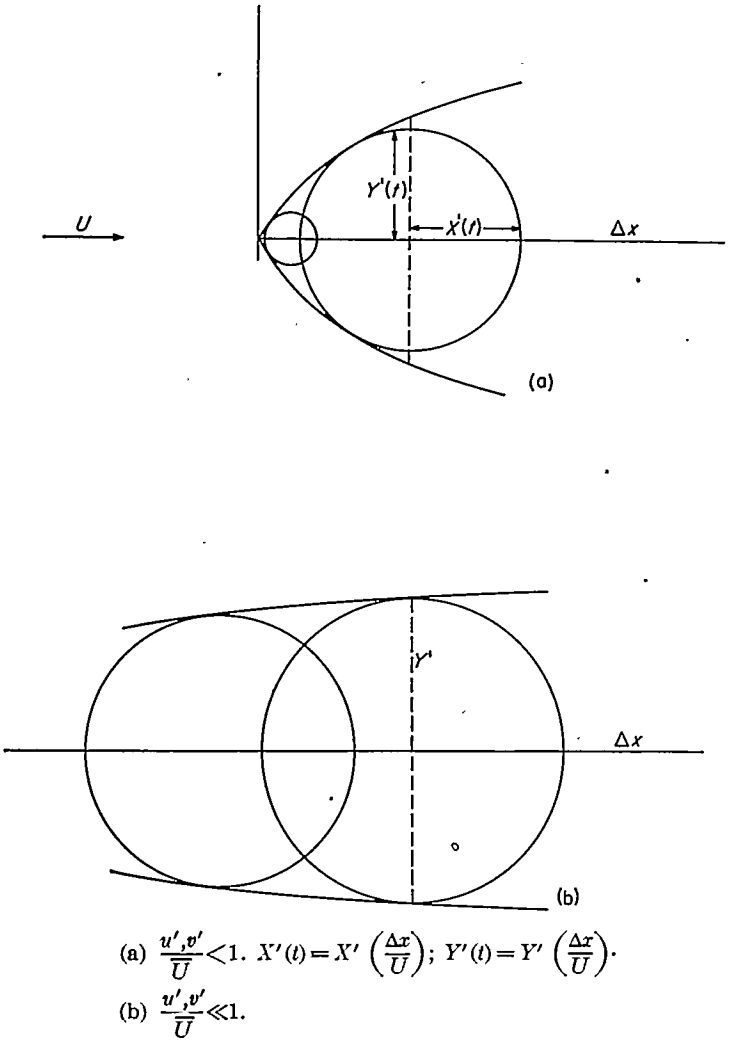

(a) $\frac{u',v'}{\overline{U}}<1$. $X'(t)=X'\left(\frac{\Delta x}{\overline{U}}\right)$; $Y'(t)=Y'\left(\frac{\Delta x}{\overline{U}}\right)$.

(b) $\frac{u',v'}{\overline{U}}\ll 1$.

FIGURE 12.—Propagation of turbulence from source moving with mean velocity $\overline{U}$.

However, it is extremely likely that if $\frac{dY'}{dx}\ll 1$ (fig. 12(b)) the mean concentration along a line Δx=Constant becomes very nearly of the same functional form as that for the source at $x=\overline{U}t$. For a zero-correlation Gaussian density, the equivalence is easily demonstrable.[3]

The condition $\frac{dY'}{dx}\ll 1$ will always occur at large enough values of Δx when $\frac{v'}{\overline{U}}<1$. This follows from the asymptotic parabolic behavior, $Y'(t)\sim\sqrt{t}$ (reference 1), of the diffusive process. It will occur for all values of Δx when $\frac{v'}{\overline{U}}\ll 1$. Therefore, in this case a simple approximate space-time transformation *in the mean* is permissible, and the t-variation in Taylor's theory of diffusion by continuous movements becomes a variation of $x/\overline{U}$. (It must be emphasized that the foregoing discussion does not apply directly to the possibility of applying a space-time transformation to the *instantaneous* turbulence variables. This latter question will be discussed later.)

In the present measurements $\frac{v'}{\overline{U}}\ll 1$, and, therefore, the Δx-variation of diffusion gives an approximate measure of the Lagrangian correlation coefficient (in time). Equation (2) can be rewritten as:

$$\overline{Y^2}\left(\frac{x}{\overline{U}}\right)=2\frac{\overline{v^2}}{\overline{U}^2}\int_0^x(x-\xi)R_v\left(\frac{\xi}{\overline{U}}\right)d\xi \qquad (8)$$

DECAYING ISOTROPIC TURBULENCE

When the turbulence is decaying in time (similar to space in the flowing turbulence) $\overline{v^2}$ is no longer constant, and the analysis cannot be carried out as far as equation (1). The same approach stops with

$$\frac{d}{dt}\overline{Y^2}=v'(t)\int_0^t v'(t-\tau)\,{}_tR_{t-\tau}\,d\tau \qquad (9)$$

where the prime denotes root-mean-square value, and

$${}_tR_{t-\tau}\equiv\frac{\overline{v(t)v(t-\tau)}}{v'(t)v'(t-\tau)}$$

There is no a priori reason to believe that ${}_tR_{t-\tau}$ is a function of τ alone, as in the nondecaying turbulent flow.

At this point Taylor (reference 2) invokes the empirical fact that over a wide range of mean velocities (all of which give essentially the same distribution of $v'/\overline{U}$ in x behind a grid) the thermal wake behind a line heat source at fixed x appears to be unchanged in form, within the experimental error. This is consistent with dependence of the diffusive process upon a variable of type

$$\eta=\int_{t_o}^t v'(t_1)\,dt_1$$
$$=\frac{1}{\overline{U}}\int_{x_o}^x v'(x_1)\,dx_1 \qquad (10)$$

Therefore, Taylor has postulated the unique dependence of ${}_tR_{t-\tau}$ on the variable η. With this postulate and the space-time transformation valid for small turbulence level, he

[3] The most general mathematical restrictions under which the superposition of a line of identical densities will yield a "cross-section" density of the same form have not been studied here. It is obvious that the condition of statistical independence is sufficient. The fact that the density of each of the velocity components in isotropic turbulence has been found to be Gaussian within the experimental precision seems to show that the equivalence under discussion is at least a good approximation.

arrives at

$$\frac{d}{dx}\overline{Y^2}=2\frac{v'}{\overline{U}}\int_0^{\eta}R_{\eta}(\eta_1)\,d\eta_1 \tag{11}$$

or

$$\frac{d}{d\eta}\overline{Y^2}=2\int_0^{\eta}R_{\eta}(\eta_1)\,d\eta_1 \tag{12}$$

where

$$d\eta=\frac{v'}{\overline{U}}\,dx$$
$$=v'dt$$

Equations (11) and (12) look like the equation for nondecaying turbulence. They also give

$$\overline{Y^2}=2\int_0^{\eta}(\eta-\eta_1)R_{\eta}(\eta_1)\,d\eta_1 \tag{13}$$

A physical significance of the length η is underscored by the limiting form of equation (13) as $\eta\to 0$ and $R_{\eta}\to 1$. Then,

$$Y'=\eta$$

so that η is a measure of the lateral diffusion that would occur if the lateral velocity fluctuation following a particle $v(t)$ remained perfectly correlated but decreased in magnitude according to the decay rate of the turbulence level.

In postulating ${}_tR_{t-\tau}=R_{\eta}(\eta)$, Taylor was apparently comparing only diffusive processes in turbulence fields with identical $\frac{v'}{\overline{U}}(x)$. Of more general interest is the comparison of diffusion in fields with differing turbulence-level distributions. Although such a generalized application of his postulate is doubtless not too well applicable, it is conceivable it might have approximate success in the more general comparison. For both convenience and lack of any obviously superior alternative, his suggestion is therefore applied in computing the results of the measurements reported here.[4]

With the η-postulate, the R_{η} Lagrangian correlation function can be obtained from measurements of $\overline{Y^2}$ as a function of Δx:

$$R_{\eta}(\eta)=\frac{1}{2}\frac{d^2}{d\eta^2}\overline{Y^2}$$
$$=\frac{1}{2}\frac{\overline{U}^2}{\overline{v^2}}\frac{d^2}{dx^2}\overline{Y^2} \tag{14}$$

A scale and a microscale can also be defined for R_{η}:

$$L_{\eta}=\int_0^{\infty}R_{\eta}(\eta_1)d\eta_1 \tag{15}$$

$$\lambda_{\eta}^2=-\frac{2}{R_{\eta}(0)''} \tag{16}$$

With nondecaying turbulence, no one-parameter true (time) Lagrangian correlation function exists, and the η-formulation is much more convenient. A further significance of this variable will appear in the comparison of Eulerian and Lagrangian treatments of diffusion from a line source in flowing turbulence.

ACCELERATIONS IN DECAYING TURBULENCE

A series expansion of $v(t+\tau)$ for decaying turbulence will show something about the initial behavior of the true (time) Lagrangian correlation function and will indicate an experimental method for examining a hypothesis of Taylor on the interchangeability of instantaneous time and space derivatives when the turbulence level is low (reference 23).

Write the Lagrangian correlation coefficient

$$R_v(t,\tau)=\frac{\overline{v(t)v(t-\tau)}}{v'(t)v'(t-\tau)} \tag{17}$$

Substitute

$$v(t-\tau)=v(t)-\left(\frac{dv}{dt}\right)_t\tau+\left(\frac{d^2v}{dt^2}\right)_t\frac{\tau^2}{2!}+\cdots$$

into numerator and denominator, and restrict the analysis to small values of τ:

$$R_v(t,\tau)\approx\frac{\overline{v^2}(t)-\frac{1}{2}\left(\frac{d\overline{v^2}}{dt}\right)_t\tau+\left[\frac{1}{2}\left(\frac{d^2\overline{v^2}}{dt^2}\right)_t-\overline{\left(\frac{dv}{dt}\right)_t^2}\right]\frac{\tau^2}{2}}{v'(t)\sqrt{\overline{v^2}(t)-\left(\frac{d\overline{v^2}}{dt}\right)_t\tau+\frac{1}{2}\left(\frac{d^2\overline{v^2}}{dt^2}\right)_t\tau^2}} \tag{18}$$

Divide numerator and denominator by $\overline{v^2}$, expand the square root in the numerator, and keep terms in τ^2:

$$R_v(t,\tau)\approx 1-\left[-\left(\frac{dv'}{dt}\right)_t^2+\overline{\left(\frac{dv}{dt}\right)_t^2}\right]\frac{\tau^2}{2\overline{v^2}(t)} \tag{19}$$

For negligible decay rate this reduces to equation (6).

Equation (19) shows that a Lagrangian microscale defined by

$$\frac{1}{\lambda_v^2(t)}=\lim_{\tau\to 0}\left[\frac{1-R_v(t,\tau)}{\tau^2}\right]$$
$$=-\left[\frac{\partial^2R_v(t,\tau)}{\partial\tau^2}\right]_{\tau=0} \tag{20}$$

is expressible as

$$\frac{1}{\lambda_v^2(t)}=\frac{1}{2\overline{v^2}}\left[\overline{\left(\frac{dv}{dt}\right)^2}-\left(\frac{dv'}{dt}\right)^2\right] \tag{21}$$

[4] After this work was completed, Dr. Batchelor suggested an alternative approximate approach: In order to construct a stationary random function out of the nonstationary $v(t)$ one first normalizes the dependent variable with its root-mean-square value. (This has been automatically accomplished by use of the correlation coefficient.) If the decaying quantity is assumed to maintain complete similarity during decay, all characteristic times (e. g., Lagrangian time scale and microscale) vary in the same way with t and the new independent variable is constructed by dividing τ by this t-variation. Unfortunately, this variation is unknown a priori, so it would be necessary to assume further that the Lagrangian scales are directly proportional to the Eulerian scales, about which there is previous experimental information. His work has now been published; see reference 22.

Introduction of Taylor's η-postulate transforms equation (19) to

$$R_\eta(\eta) \approx 1 - \left[\overline{\left(\frac{dv}{d\eta}\right)^2}_{\eta=0} - \left(\frac{dv'}{d\eta}\right)^2_{\eta=0}\right] \frac{\eta^2}{2\overline{v^2}_{\eta=0}} \tag{22}$$

after the additional approximation that $v'(\eta) \approx v'(0)$ when η is very small.

This gives a new expression for Lagrangian microscale λ_η:

$$\frac{1}{\lambda_\eta^2} = \frac{1}{2\overline{v^2}}\left[\overline{\left(\frac{dv}{d\eta}\right)^2} - \left(\frac{dv'}{d\eta}\right)^2\right] \tag{23}$$

Equation (23) is in contradiction to equation (17) of part IV of reference 2. In that work Taylor has apparently assumed that v' is a nondecaying function of η. However it certainly is decaying, even in terms of this distorted coordinate, and the $dv'/d\eta$-term must be included.

Since λ_η and $v'(x)$ can be determined experimentally from the mean thermal wake behind a line heat source, equation (23) permits determination of $\overline{\left(\frac{dv}{d\eta}\right)^2}$ which is simply related to the mean-square "Stokes" acceleration $\overline{\left(\frac{dv}{dt}\right)^2} = (v')^2 \overline{\left(\frac{dv}{d\eta}\right)^2}$. This quantity is of particular interest for the possibility of an instantaneous space-time transformation at low turbulence levels. This was first proposed by Taylor (reference 23) and has since been used very widely, especially to get approximate values of partial derivatives with respect to x (the mean-flow direction) by measurements of time partial derivatives.

The total (or Stokes) derivative of $v(x, y, z, t)$ in a turbulent flow with mean velocity $\overline{U}$ along the x-direction is

$$\frac{dv}{dt} = \frac{\partial v}{\partial t} + (\overline{U}+u)\frac{\partial v}{\partial x} + v\frac{\partial v}{\partial y} + w\frac{\partial v}{\partial z} \tag{24}$$

Taylor's hypothesis amounts to the statement that

$$\frac{\partial v}{\partial t} \approx -\overline{U}\frac{\partial v}{\partial x}$$

or

$$\frac{\partial v}{\partial t} = -U\frac{\partial v}{\partial x} + \epsilon \tag{24a}$$

with

$$\left[\frac{\overline{\epsilon^2}}{\overline{U}^2\overline{\left(\frac{\partial v}{\partial x}\right)^2}}\right]^{1/2} \ll 1 \tag{25}$$

In detail, equation (25) is

$$\left[\frac{\overline{\left(\frac{dv}{dt}\right)^2} + u_i u_j \frac{\partial v}{\partial x_i}\frac{\partial v}{\partial x_j} - 2\overline{u_i \frac{dv}{dt}\frac{\partial v}{\partial x_i}}}{\overline{U}^2\overline{\left(\frac{\partial v}{\partial x}\right)^2}}\right]^{1/2} \ll 1 \tag{25a}$$

In the absence of information on the algebraic sign of the triple correlation term, it is sufficient to require the two conditions.[5]

$$\left.\begin{aligned}\left[\frac{\overline{\left(\frac{dv}{dt}\right)^2}}{\overline{U}^2\overline{\left(\frac{\partial v}{\partial x}\right)^2}}\right]^{1/2} &\ll 1 \\ \left[\frac{u_i u_j \frac{\partial v}{\partial x_i}\frac{\partial v}{\partial x_j}}{\overline{U}^2\overline{\left(\frac{\partial v}{\partial x}\right)^2}}\right]^{1/2} &\ll 1\end{aligned}\right\} \tag{26}$$

But $\overline{\left(\frac{dv}{dt}\right)^2}$ can be determined from measurements of $Y'(x)$; $\overline{\left(\frac{\partial v}{\partial x}\right)^2} = 2\frac{\overline{v^2}}{\lambda^2}$, where λ is the Eulerian microscale (reference 2); and upper bounds, in terms of measurable functions, can be set on $\overline{u_i u_j \frac{\partial v}{\partial x_i}\frac{\partial v}{\partial x_j}}$ with the use of Schwarz inequalities. Thus, an experimental check of the requirements in equation (26) is to be made in the section entitled "Computation of Results."

RELATION BETWEEN EULERIAN AND LAGRANGIAN MICROSCALES

Taylor (reference 2) inferred an approximate relation between λ_η and λ by neglecting the effect of viscosity on pressure-gradient fluctuations and estimating $\left[\overline{\left(\frac{\partial p}{\partial y}\right)^2}\right]^{1/2}$ as being approximately $3\rho\left[v^2\overline{\left(\frac{\partial v}{\partial y}\right)^2}\right]^{1/2}$. This led to a constant ratio λ_η/λ for all turbulence. The rough nature of this analysis induced Heisenberg (reference 25) to conduct a more detailed study of the static-pressure fluctuations and to reestimate the λ_η/λ ratio. However, he followed Taylor in ignoring the $dv'/d\eta$-term in the relation between λ_η and $\overline{\left(\frac{dv}{d\eta}\right)^2}$ (see equation (23)) and in neglecting viscous terms in the relation between λ_η and $\overline{\left(\frac{\partial p}{\partial y}\right)^2}$.

Although these omissions are probably not serious except in the low Reynolds number range, it seems interesting, if only for the sake of completeness, to use a Heisenberg type of approximation for $\overline{\left(\frac{\partial p}{\partial y}\right)^2}$ and to repeat his treatment with the omissions rectified.

---

[5] Lin has discussed the validity of Taylor's hypothesis using a slightly different formulation in reference 24. He points out there that if $A = \sum_1^n a_r$, then (from the Schwarz inequality $\overline{(A^2)}^{1/2} \leq \sum_1^n \overline{(a_r^2)}^{1/2}$ where a_r is a set of numbers.

From the complete Navier-Stokes equations in the wave-number space, Heisenberg deduced an approximate expression for $\overline{(\nabla p)^2}$ in terms of mean quadruple products of the "harmonics" of the velocity field. His principal simplifying assumptions were:

(a) Different Fourier components of the velocity field are uncorrelated

(b) The turbulent energy spectrum is given by the solution to his equilibrium-energy-transfer equation, above a lower cut-off wave number k_0

Following these, but using Chandrasekhar's (reference 26) solution to the Heisenberg equation instead of the interpolation formula used by Heisenberg, there results

$$\overline{\left(\frac{\partial p}{\partial y}\right)^2}=\frac{25.2}{\kappa}\rho^2\nu\frac{(v')^3}{\lambda^3} \tag{27}$$

where κ is a dimensionless empirical constant.

The numerical constant in equation (27) would perhaps have been given more accurately by the use of a "self-preserving" spectrum (calculated by Chandrasekhar from Heisenberg's equation) instead of the stationary spectrum with low cut-off wave number. Time was not taken to make the requisite additional calculations because: (a) The value of $\overline{\left(\frac{\partial p}{\partial y}\right)^2}$ depends principally upon the high-wave-number region of the velocity spectrum rather than the low-wave-number region, where the difference would be greatest, and (b) the experimental results and (especially) the value of κ both have a considerable range of uncertainty.

The mean square of the y-component of the Navier-Stokes equation will lead to a relation between λ_η and λ:

$$\frac{dv}{dt}=\frac{\partial v}{\partial t}+u\frac{\partial v}{\partial x}+v\frac{\partial v}{\partial y}+w\frac{\partial v}{\partial z}$$

$$=-\frac{1}{\rho}\frac{\partial p}{\partial y}+\nu\nabla^2 v$$

therefore,

$$\overline{\left(\frac{dv}{dt}\right)^2}=\frac{1}{\rho^2}\overline{\left(\frac{\partial p}{\partial y}\right)^2}+\nu^2\overline{(\nabla^2 v)^2} \tag{28}$$

where the correlation between pressure gradient and velocity Laplacian function is zero because of isotropy.

Equations (23) and (27) give the first two terms in terms of the microscales, and the mean-square Laplacian function is expressible in terms of the fourth derivative of the Von Kármán-Howarth $f(r)$ correlation coefficient at $r=0$ (reference 27):

$$\overline{(\nabla^2 v)^2}=\frac{35}{3}(v')^2 f^{iv}(0) \tag{29}$$

Consequently, equation (28) becomes

$$2\frac{(v')^4}{\lambda_\eta^2}+\left(\frac{dv'}{dt}\right)^2=\frac{25.2}{\kappa}\nu\frac{(v')^3}{\lambda^3}+\frac{35}{3}\nu^2(v')^2 f^{iv}(0)$$

The second term in this equation can be replaced by the turbulence-decay equation

$$\frac{d(v')^2}{dt}=-10\nu\frac{(v')^2}{\lambda^2} \tag{30}$$

whence

$$\frac{dv'}{dt}=-5\nu\frac{v'}{\lambda^2}$$

so that

$$2\frac{(v')^4}{\lambda_\eta^2}+25\nu^2\frac{(v')^2}{\lambda^4}=\frac{25.2}{\kappa}\nu\frac{(v')^3}{\lambda^3}+\frac{35}{3}\nu^2(v')^2 f^{iv}(0)$$

therefore,

$$\frac{\lambda^2}{\lambda_\eta^2}=\frac{12.6}{\kappa}\frac{1}{R_\lambda}-\frac{12.5}{R_\lambda^2}+\frac{35}{6}f^{iv}(0)\frac{\nu^2\lambda^2}{(v')^2} \tag{31}$$

where $R_\lambda=\frac{v'\lambda}{\nu}$.

Batchelor and Townsend (reference 19) have deduced an expression for $f^{iv}(0)$ which is valid in the region of decay where both $1/(v')^2$ and λ^2 increase linearly with t (corresponding to large values of R_λ):

$$\lambda^4 f^{iv}(0)=\frac{30}{7}+\frac{1}{2}R_\lambda S \tag{32}$$

where $S=-\overline{\left(\frac{\partial v}{\partial y}\right)^3}\Big/\left[\overline{\left(\frac{\partial v}{\partial y}\right)^2}\right]^{3/2}$, the skewness factor. Their experimental results showed $S=0.39$ approximately constant for isotropic turbulence. Then the estimate for λ/λ_η becomes

$$\left(\frac{\lambda}{\lambda_\eta}\right)^2=\frac{12.5}{R_\lambda^2}+\left(\frac{12.6}{\kappa}+1.14\right)\frac{1}{R_\lambda} \tag{33}$$

The value of κ was first estimated by Heisenberg (reference 25), from measurements of turbulence decay, as 0.85. This method may be regarded as emphasizing the (relatively low wave number) energy-bearing range of the spectrum. Lee (reference 28) worked out an estimate based upon skewness factor ($\kappa=0.13$), which gives heavy weight to the high-wave-number range. Proudman (reference 29) has reestimated κ by comparison with measured curves of the double and triple velocity correlations. The value $\kappa=0.45$ leads to reasonably good agreement for the moderately high-wave-number region, over a wide range of values of R_λ.

It may be remarked that the supposed constancy of κ is merely a postulate of the Heisenberg dimensional formulation of the spectral transfer function. In fact it is by no means obvious that this turbulent part of the transfer is quantitatively independent of the amount of spectrally local dissipation to heat. In any case, Proudman's estimate of $\kappa=0.45$ has been used here. Therefore,

$$\left(\frac{\lambda}{\lambda_\eta}\right)^2=\frac{12.5}{R_\lambda^2}+\frac{29}{R_\lambda} \tag{34}$$

In the limit of $R_\lambda \to 0$, equation (34) does not apply since equation (32) does not apply. However, the appropriate

limiting relation can be obtained directly. In this limiting condition the pressure term in equation (28) is negligible compared with the viscous term (the former goes with $1/R_\lambda$ and the latter with $1/R_\lambda^2$), and the Eulerian velocity correlation coefficient is (reference 27) $f(r)=e^{-r^2/x^2}$. This gives $f^{iv}(0)=3/\lambda^4$ and

$$\left(\frac{\lambda}{\lambda_y}\right)^2=\frac{3.5}{R_\lambda^2} \tag{35}$$

EULERIAN ANALYSIS OF HEAT DIFFUSION FROM A LINE SOURCE

The two-dimensional turbulent-heat-transfer equation is

$$\overline{U}\frac{\partial\bar{\theta}}{\partial x}+\overline{V}\frac{\partial\bar{\theta}}{\partial y}=\frac{k}{\rho c_p}\left(\frac{\partial^2\bar{\theta}}{\partial x^2}+\frac{\partial^2\bar{\theta}}{\partial y^2}\right)-\frac{\partial}{\partial x}(\overline{\vartheta u})-\frac{\partial}{\partial y}(\overline{\vartheta v}) \tag{36}$$

where $\bar{\theta}$ is mean temperature, ϑ is temperature fluctuation about the mean, k is thermal conductivity, and c_p is specific heat at constant pressure.

For the thermal wake behind a line source in isotropic turbulence with constant mean velocity $\overline{V}=0$. With restriction to low turbulence level, a "boundary-layer" type of approximation can be applied to the mean wake, so that

$$\frac{\partial^2\bar{\theta}}{\partial x^2}\ll\frac{\partial^2\bar{\theta}}{\partial y^2}$$

and

$$\frac{\partial}{\partial x}(\overline{\vartheta u})\ll\overline{U}\frac{\partial\bar{\theta}}{\partial x}$$

so that equation (36) takes the approximate form

$$\overline{U}\frac{\partial\bar{\theta}}{\partial x}=\frac{k}{\rho c_p}\frac{\partial^2\bar{\theta}}{\partial y^2}-\frac{\partial}{\partial y}(\overline{\vartheta v}) \tag{37}$$

It must be emphasized that for this particular initial condition on the temperature (effectively a "point source"), the restriction to small turbulence level $v'/\overline{U}\ll1$ does *not* imply that $\vartheta'/\bar{\theta}$ is small. In fact, for this problem $\vartheta'/\bar{\theta}$ is often greater than unity, especially at the "edge" of the mean wake, as has been discussed in reference 10 and will be brought out again later in the present report.

When the molecular transport can be neglected relative to turbulent transport

$$\overline{U}\frac{\partial\bar{\theta}}{\partial x}=-\frac{\partial}{\partial y}(\overline{\vartheta v}) \tag{38}$$

an equation given in reference 10; a slightly more general treatment follows:

With a constant rate of heat generation (similar to steady state in the average), the application of a Von Kármán integral-relation treatment to equation (38) yields an integral condition:

$$2\rho c_p\overline{U}\int_0^\infty\bar{\theta}\,dy=\text{Constant}=H \tag{39}$$

where H is the average time rate at which heat crosses all planes perpendicular to $\overline{U}$ per unit length of heat source (z-direction). Of course, $\overline{\vartheta u}$ has been neglected relative to $\overline{\theta U}$ in equation (39).

Equation (38) has two unknowns, and the first objective is to express $\overline{\vartheta v}$ as a function of the (more easily measurable) $\overline{\theta}(x,y)$. After integration with respect to y,

$$\overline{\vartheta v}=-\overline{U}\int_0^y\frac{\partial\bar{\theta}}{\partial x}\,dy+F(x)$$

But, by symmetry, $\overline{\vartheta v}=0$ for $y=0$. Hence $F(x)=0$ and

$$\overline{\vartheta v}=-\overline{U}\int_0^y\frac{\partial\bar{\theta}}{\partial x}\,dy \tag{40}$$

This relation is sufficient for the computation of $\overline{\vartheta v}(x,y)$ from the measured $\overline{\theta}(x,y)$ but the empirical fact of simple geometrical similarity in $\overline{\theta}(x,y)$ suggests exploitation of the consequent simplification.

Assume

$$\bar{\theta}(x,y)=\bar{\theta}_o(x)f(\xi) \tag{41}$$

where $\xi=y/Y'(x)$. This transforms equation (39) to

$$\bar{\theta}_o(x)Y'(x)=\frac{H^*}{\overline{U}} \tag{42}$$

where $H^*=\dfrac{H}{2\rho c_p\displaystyle\int_0^\infty f(\xi)\,d\xi}=\text{Constant}$. It transforms equation (40) to

$$\overline{\vartheta v}=\left(-\overline{U}\int_0^\xi f(\xi)\,d\xi\right)Y'(x)\frac{d\bar{\theta}_o}{dx}+\left(\overline{U}\int_0^\xi\xi\frac{df}{d\xi}\,d\xi\right)\bar{\theta}_o(x)\frac{dY'}{dx} \tag{43}$$

With equation (42), $\bar{\theta}_o(x)$ can be eliminated from equation (43), and after integration of the dimensionless integrals this leads to the final form for the turbulent-heat-transfer correlation,

$$\overline{\vartheta v}(x,y)=H^*\xi f(\xi)\frac{1}{Y'(x)}\frac{dY'}{dx} \tag{44}$$

where

$$\xi=\frac{y}{Y'(x)}$$

The same sort of analysis can be made on equation (37) which includes the molecular conduction, but the rather large experimental scatter in the present measurements seems to make such a refinement inappropriate.

An "exchange" coefficient or "diffusion" coefficient for turbulent heat transfer k_T is simply expressible in terms of $\bar{\theta}(x,y)$. A conventional procedure for semiempirical analyses is to write for the turbulent transport an expression just like that for the molecular transport:

$$-\rho c_p\overline{\vartheta v}=k_T\frac{\partial\bar{\theta}}{\partial y} \tag{45}$$

which serves as the definition of k_T.

For the simple case of equation (44), it turns out that

$$k_T=\rho c_p\overline{U}\left[\frac{\xi f(\xi)}{\frac{df}{d\xi}}\right]Y'(x)\frac{dY'}{dx} \tag{46}$$

This has the particularly interesting property that in a nondecaying turbulence at very large values of x, where the mean thermal wake spreads parabolically (reference 1), k_T becomes independent of explicit dependence on x.

A more startling simplification follows for a particular mean temperature distribution across the wake: All dependence of k_T on y disappears if

$$\frac{df}{d\xi}\propto\xi f$$

that is, if

$$f(\xi)=e^{-\frac{1}{2}\xi^2} \tag{47}$$

But this is the Gaussian function, which is found empirically to fit all the measurements within the experimental scatter. Hence one arrives at the empirical result that in both nondecaying and decaying turbulence k_T is independent of y in the thermal wake behind a line source of heat. From equation (47), $\frac{df}{d\xi}=-\xi f(\xi)$ and

$$k_T=\rho c_p\overline{U}Y'(x)\frac{dY'}{dx} \tag{48}$$

It can be seen that in the nondecaying case at very large values of x, k_T is constant and independent of both y and x.

RELATION BETWEEN SOME LAGRANGIAN AND EULERIAN PARAMETERS IN TRANSPORT

There has apparently been little effort to relate the Eulerian and Lagrangian formulations of turbulent diffusion up to the present time. Exceedingly simple boundary conditions permit some connection to be made in restricted ranges of the present problem.

For nondecaying or (with much less accuracy) decaying turbulence, equation (13) applies:

$$\overline{Y^2}=2\int_0^\eta(\eta-\eta_1)R_\eta(\eta_1)d\eta_1$$

or, equation (12),

$$\frac{d\overline{Y^2}}{d\eta}=2Y'\frac{dY'}{d\eta}$$

$$=2\int_0^\eta R_\eta(\eta_1)d\eta_1$$

For small values of η, $R_\eta=1-\frac{\eta^2}{\lambda_\eta^2}$ whence

$$\overline{Y^2}=\eta^2\left(1-\frac{1}{6}\frac{\eta^2}{\lambda_\eta^2}\right) \tag{49}$$

$$\frac{d\overline{Y^2}}{d\eta}=2\eta\left(1-\frac{1}{3}\frac{\eta^2}{\lambda_\eta^2}\right) \tag{50}$$

Substituted into equation (44) these give

$$\overline{\vartheta v}=H^*f(\xi)\frac{y}{\eta^2}\left(1-\frac{1}{12}\frac{\eta^2}{\lambda_\eta^2}\right)\frac{v'}{\overline{U}} \tag{51}$$

while equation (46) becomes

$$k_T=\rho c_p v'y\frac{f(\xi)}{df/d\xi}\left(1-\frac{1}{4}\frac{\eta^2}{\lambda_\eta^2}\right) \tag{52}$$

where $\eta=\frac{1}{\overline{U}}\int_0^x v'dx$ and $\xi=\frac{y}{\overline{Y'(x)}}\approx\frac{y}{\eta}\left(1+\frac{1}{12}\frac{\eta^2}{\lambda_\eta^2}\right)$. In fact, for small values of η, $\eta\approx\frac{v'}{\overline{U}}x$.

For low-level nondecaying turbulence, $\eta=\frac{v'}{\overline{U}}x$, and equation (51) becomes

$$\overline{\vartheta v'}=H^*f(\xi)\frac{y}{x^2}\left(1-\frac{1}{12}\frac{\overline{v^2}}{\overline{U^2}}\frac{x^2}{\lambda_\eta^2}\right)\frac{\overline{U}}{v'} \tag{53}$$

while equation (52) becomes

$$k_T=\rho c_p v'y\frac{f(\xi)}{df/d\xi}\left(1-\frac{1}{4}\frac{\overline{v^2}}{\overline{U^2}}\frac{x^2}{\lambda_\eta^2}\right) \tag{54}$$

As $\eta\to0$ both equations (51) and (53) reduce to

$$\overline{\vartheta v}=H^*f(\xi)\frac{\overline{U}}{v'}\frac{y}{x^2} \tag{55}$$

while equations (52) and (54) reduce to

$$k_T=\rho c_p v'\frac{f(\xi)}{df/d\xi}y \tag{56}$$

At the other extreme, when η is very large,

$$\overline{Y^2}=2\eta L_\eta-2M_1 \tag{57}$$

where $M_1=\int_0^\infty\eta R_\eta(\eta)\,d\eta=$Constant and

$$\frac{d\overline{Y^2}}{d\eta}=2L_\eta \tag{58}$$

In this case,

$$\overline{\vartheta v}=H^*f(\xi)\frac{yL_\eta\frac{v'}{\overline{U}}}{[2(\eta L_\eta-M_1)]^{3/2}} \tag{59}$$

and

$$k_T=\rho c_p v'\frac{f(\xi)}{df/d\xi}\frac{yL_\eta}{[2(\eta L_\eta-M_1)]^{1/2}} \tag{60}$$

As indicated previously, the η-variation can be expressed

in terms of x or t.

If η is allowed to become large enough to make $yL_\eta \gg M_1$

$$\overline{\vartheta v}=H^* f(\xi)\frac{y\dfrac{v'}{\overline{U}}}{2^{3/2}\eta^{3/2}L_\eta^{1/2}} \tag{61}$$

$$k_T=\rho c_p v' \frac{f(\xi)}{df/d\xi} y\left(\frac{L_\eta}{2\eta}\right)^{1/2} \tag{62}$$

The above formulas take on particularly simple forms if the empirical result of a Gaussian $f(\xi)$ is utilized:

$$f(\xi)=e^{-\frac{1}{2}\xi^2}$$

Then the general expressions for $\overline{\vartheta v}$ and k_T (equations (44) and (46)) become

$$\overline{\vartheta v}(x,y)=\frac{H^*}{(Y')^2(x)}\frac{dY'}{dx}ye^{-\frac{1}{2}\left(\frac{y}{Y'}\right)^2} \tag{63}$$

and

$$k_T(x,y)=\rho c_p Y'(x)\frac{dY'}{dx}\overline{U} \tag{64}$$

the latter having been deduced in the previous section. The particular forms for small values of η would follow from substitution of equations (49) and (50) into these two.

However, the most interesting form occurs for very large values of η. There $Y'(x)$ is given by equation (57) and

$$\overline{\vartheta v}(x,y)=\frac{H^* yL_\eta\dfrac{v'}{\overline{U}}}{[2(\eta L_\eta-M_1)]^{3/2}}\exp\left(\frac{-\frac{1}{4}y^2}{\eta L_\eta-M_1}\right) \tag{65}$$

$$k_T(x,y)=\rho c_p v' L_\eta=\text{Constant} \tag{66}$$

For still larger values of η, such that $M_1 \ll \eta L_\eta$,

$$\overline{\vartheta v}(x,y)=\frac{H^*}{2\sqrt{2}}\frac{y\dfrac{v'}{\overline{U}}}{\eta^{3/2}L_\eta^{1/2}}\exp\left(-\frac{1}{4}\frac{y^2}{\eta L_\eta}\right) \tag{67}$$

and

$$k_T(x,y)=\rho c_p v' L_\eta=\text{Constant}$$

The constancy of k_T for large values of η (large values of t or x) is to be expected; a treatment of molecular diffusion by this method must certainly yield a constant coefficient for times much larger than the mean free time (of flight) of the molecules—that is, for all "macroscopic times." Put another way, the simple parabolic behavior of Y' for large values of η is a sure indication that $\bar{\Theta}$ obeys the simple classical diffusion equation with constant coefficient, when viewed extremely "coarsely."

Perhaps the chief interest of equation (66) is its identification of L_η as a significant Lagrangian length for diffusion at a large distance from the source. It enters the expression for turbulent-diffusion coefficient in much the same way as mean free path enters the expressions for the molecular-diffusion coefficients. Furthermore, its role appears to be much like that attributed to Prandtl's "mixing length," which was brought into the turbulent-transport problem in a more or less intuitive fashion.

Of course, the possible crude nature of Taylor's original η-postulate may render the significance of L_η more qualitative than quantitative in the case of decaying turbulence.

COMPUTATION OF RESULTS

Although Taylor's assumption of the unique dependence of ${}_tR_{t-\tau}$ upon η is not likely to be accurate for collapsing together cases with widely differing turbulence decay rates, it does provide a relatively simple relation between $Y'(x)$ and $R_\eta(\eta)$. Therefore all of the mean-thermal-wake data were reduced on the η-basis.

In principle the complete $R_\eta(\eta)$ curve can be obtained from $\overline{Y^2}(x)$ by double differentiation (equation (12)):

$$R_\eta=\frac{1}{2}\frac{d^2}{d\eta^2}(\overline{Y^2}) \tag{68}$$

or

$$R_\eta=\frac{1}{2}\left(\frac{\overline{U}}{v'}\right)^2\frac{d^2}{dx^2}(\overline{Y^2})$$

However, simple double differentiation of the squares of a curve as uncertain as $Y'(x)$ seems almost hopelessly indeterminate—although Taylor (reference 2) and Collis (reference 7) have apparently followed this procedure. A somewhat more circumspect technique has been tried here: The values of λ_η and L_η were determined first, through certain limit relations (to be described). Then the R_η curve was determined by double differentiation, subject to the restrictions of agreement with the previously determined scales. Thanks to rather poor determinancy of values of λ_η and L_η this method is not so much of an improvement as it might first appear.

LAGRANGIAN MICROSCALE λ_η

If equation (13) is restricted to very small values of η the parabolic approximation for R_η can be introduced:

$$\overline{Y^2}=2\int_0^\eta(\eta-\eta_1)\left(1-\frac{\eta_1^2}{\lambda_\eta^2}\right)d\eta_1 \tag{69}$$

therefore

$$\frac{\overline{Y^2}}{\eta^2}=1-\frac{1}{6}\frac{\eta^2}{\lambda_\eta^2}$$

whence

$$\lambda_\eta^2=-\frac{1}{6}\left[\frac{d}{d(\eta^2)}\left(\frac{\overline{Y^2}}{\eta^2}\right)\right]_{\eta^2\to 0} \tag{70}$$

The computational procedure was to plot $\overline{Y^2}/\eta^2$ against η^2 and to estimate the slope of the faired curve at $\eta=0$ where the curve must pass through unity. The abscissa intercept of the 0-tangent is $6\lambda_\eta^2$. The actual points, faired curves,

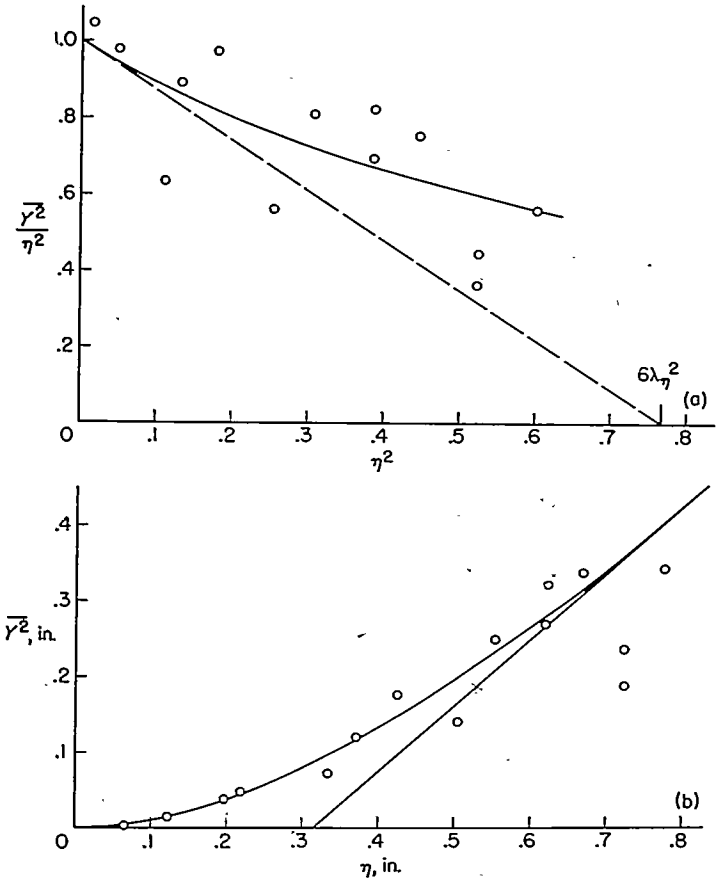

(a) λ_η=0.36.
(b) L_η=0.43.

FIGURE 13.—Determination of λ_η and L_η; $\frac{x_o}{M}$=43.4, M=1 inch, and $\overline{U}$=8.5 feet per second.

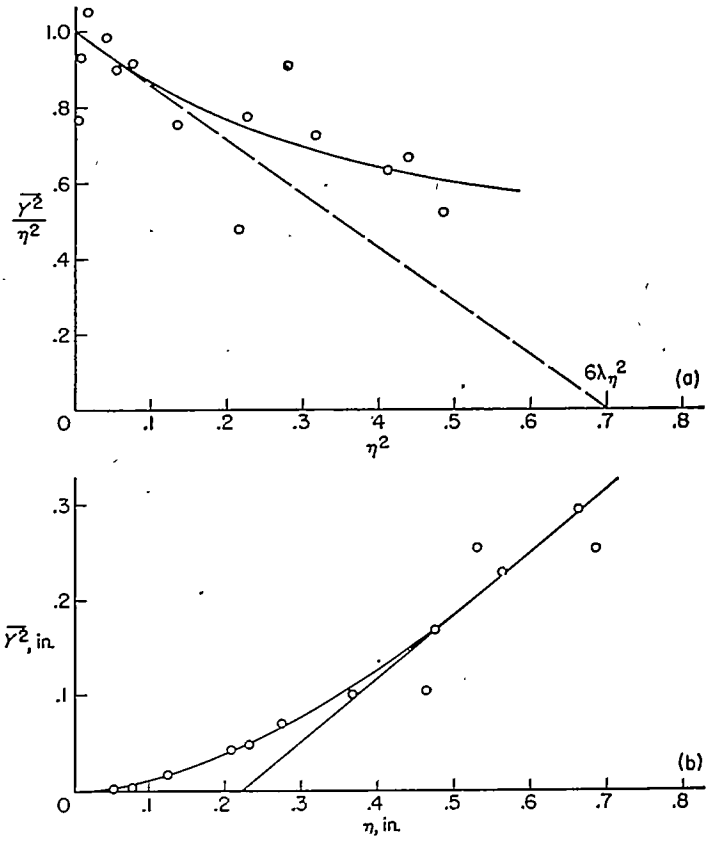

(a) λ_η=0.34.
(b) L_η=0.33.

FIGURE 14.—Determination of λ_η and L_ρ; $\frac{x_o}{M}$=43.4, M=1 inch, and $\overline{U}$=25.6 feet per second.

and tangents for all cases are presented in figures 13 to 22. Clearly the precision is poor.

LAGRANGIAN SCALE L_η

Consider equation (12) in the limit as $\eta \to \infty$. It immediately gives

$$L_\eta = \frac{1}{2} \lim_{\eta \to \infty} \left(\frac{d\overline{Y^2}}{d\eta} \right) \tag{71}$$

and the graphical procedure based on this is also presented in figures 13 to 22. Some of the asymptotic slopes drawn are not the best representation of the experimental points. This is due to the auxiliary (assumed) restriction that R_η cannot increase with increasing values of η as long as R_η has not previously dropped below zero. The graphical precision attainable is perhaps a little better here than that for λ_η^2, but the square root necessary to get λ_η means that λ_η is determined about as well as is L_η.

LAGRANGIAN CORRELATION FUNCTION $R_\eta(\eta)$

With λ_η and L_η determined, the initial (small Δx) and final (large Δx) behavior of the curve $Y'(\Delta x)$ is prescribed. These parts of the curve were drawn on a graph with the experimental points. Then the fairing in of a reasonable central portion to this mean $Y'(\Delta x)$ curve was a relatively simple matter. The R_η curve was then obtained by double differentiation.

The curves drawn for $Y'(\Delta x)$ in figures 23 to 32 were determined in the fashion described above, as were the curves for R_η in the same figures.

EULERIAN MICROSCALE λ

In view of the approximate nature of the determination of λ_η, no new direct measurements were made of the Eulerian microscale λ. Instead, λ was computed with the energy

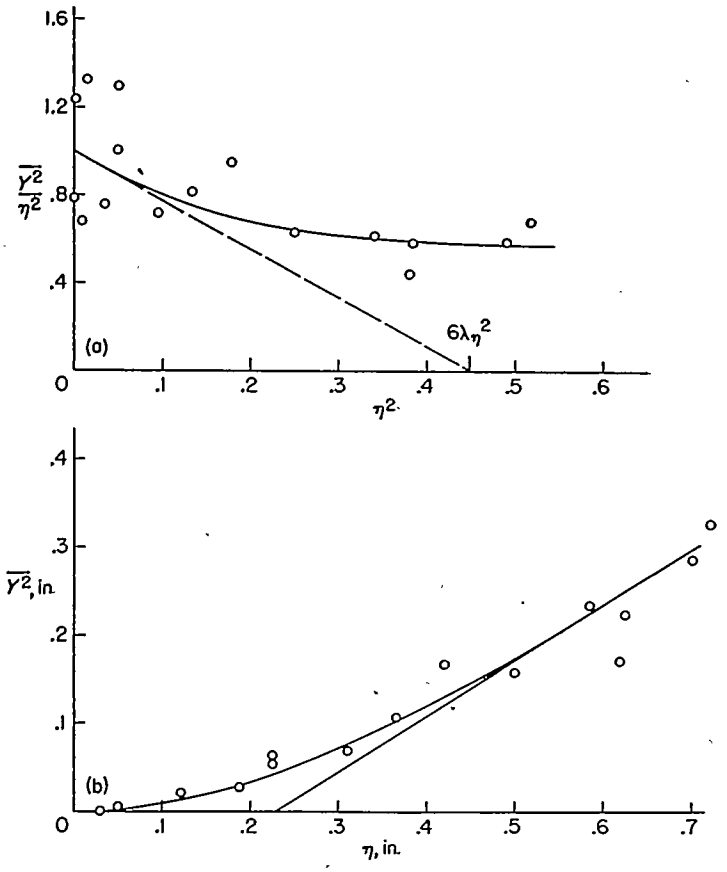

(a) $\lambda_\eta=0.27$.
(b) $L_\eta=0.33$.

FIGURE 15.—Determination of λ_η and L_η; $\frac{x_o}{M}=43.4$, $M=1$ inch, and $\overline{U}=38$ feet per second.

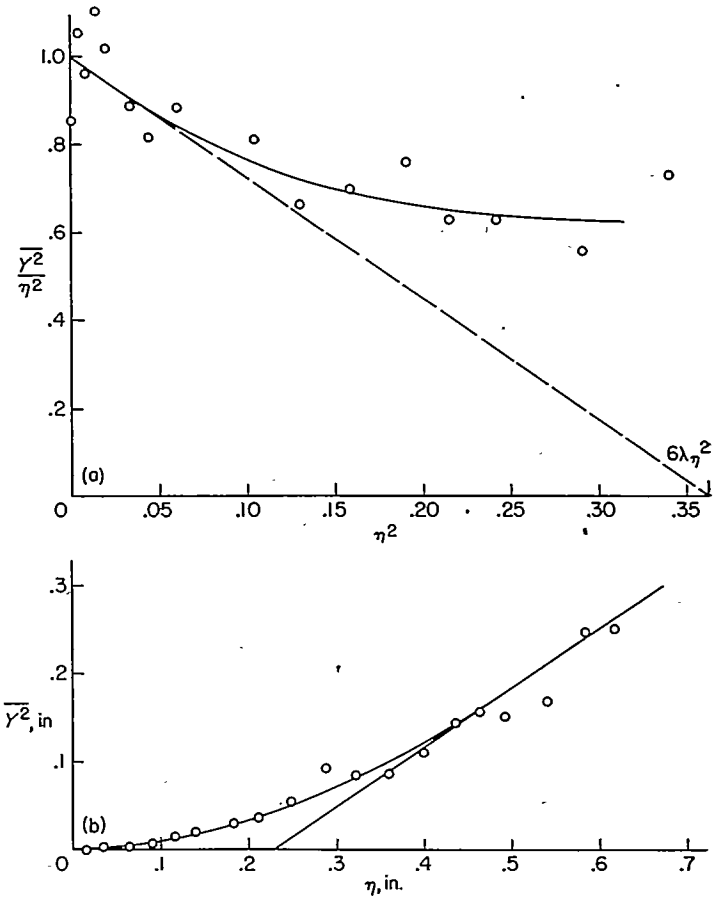

(a) $\lambda_\eta=0.25$.
(b) $L_\eta=0.34$.

FIGURE 16.—Determination of λ_η and L_η; $\frac{x_o}{M}=43.4$, $M=\frac{1}{2}$ inch, and $\overline{U}=25.6$ feet per second.

equation for isotropic turbulence, from the measurements of turbulence decay:

$$\lambda^2=-10\nu\frac{\overline{v^2}}{d\overline{v^2}/dt} \tag{72}$$

or, with the space-time transformation,

$$\lambda^2=-10\nu\frac{\overline{v^2}}{\overline{U}\dfrac{d\overline{v^2}}{dx}} \tag{73}$$

EULERIAN SCALE L

Earlier investigations have shown that the Eulerian scale in a grid-produced turbulence is closely a linear function of the mesh size of the grid producing the turbulence (for a given value of x and grid geometry) and is not significantly dependent upon the mean velocity (or grid Reynolds number, provided it is sufficient to cause turbulence). Therefore the values of L have been deduced from earlier measurements at the California Institute of Technology (reference 18) on grids of essentially the same geometry.

Table I summarizes the results for Lagrangian and Eulerian scales and microscales. The results have been grouped to show the effect of systematic variation of one parameter at a time. Some of the results are presented in figures 33, 34, and 35.

INSTANTANEOUS SPACE-TIME TRANSFORMATION

The permissibility of an instantaneous space-time transformation in flowing turbulence,

$$\frac{\partial v}{\partial x}\approx-\frac{1}{\overline{U}}\frac{\partial v}{\partial t} \tag{74}$$

can be estimated in accordance with equations (26). For equation (74) to be valid, the sufficient requirements are those given in equations (26) that:

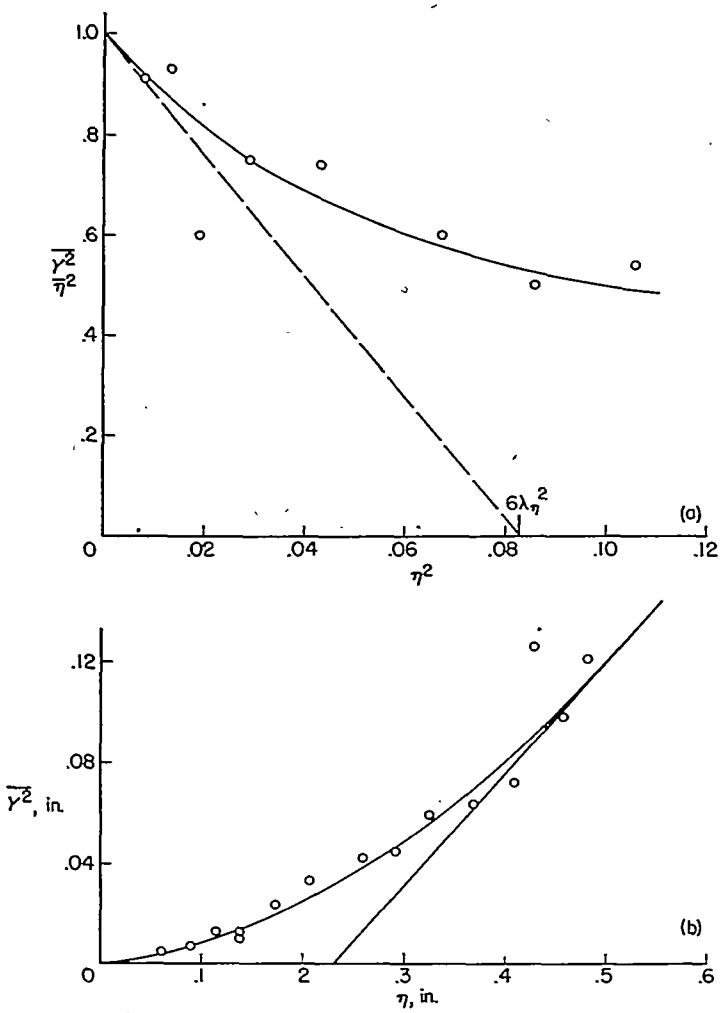

(a) $\lambda_\eta=0.12$.
(b) $L_\eta=0.21$.

FIGURE 17.—Determination of λ_η and L_η; $\frac{x_o}{M}=43.4$, $M=\frac{1}{4}$ inch, and $\overline{U}=25.6$ feet per second.

$$T\equiv\left[\frac{\overline{\left(\frac{dv}{dt}\right)^2}}{\overline{U}^2\overline{\left(\frac{\partial v}{\partial x}\right)^2}}\right]^{1/2}\ll 1$$

$$\left[\frac{u_i u_j\frac{\partial v}{\partial x_i}\frac{\partial v}{\partial x_j}}{\overline{U}^2\overline{\left(\frac{\partial v}{\partial x}\right)^2}}\right]^{1/2}\ll 1$$

With the aid of equation (23), the turbulence decay equation, and the Taylor relation $\overline{\left(\frac{\partial v}{\partial x}\right)^2}=2\frac{\overline{v^2}}{\lambda^2}$, the first of these

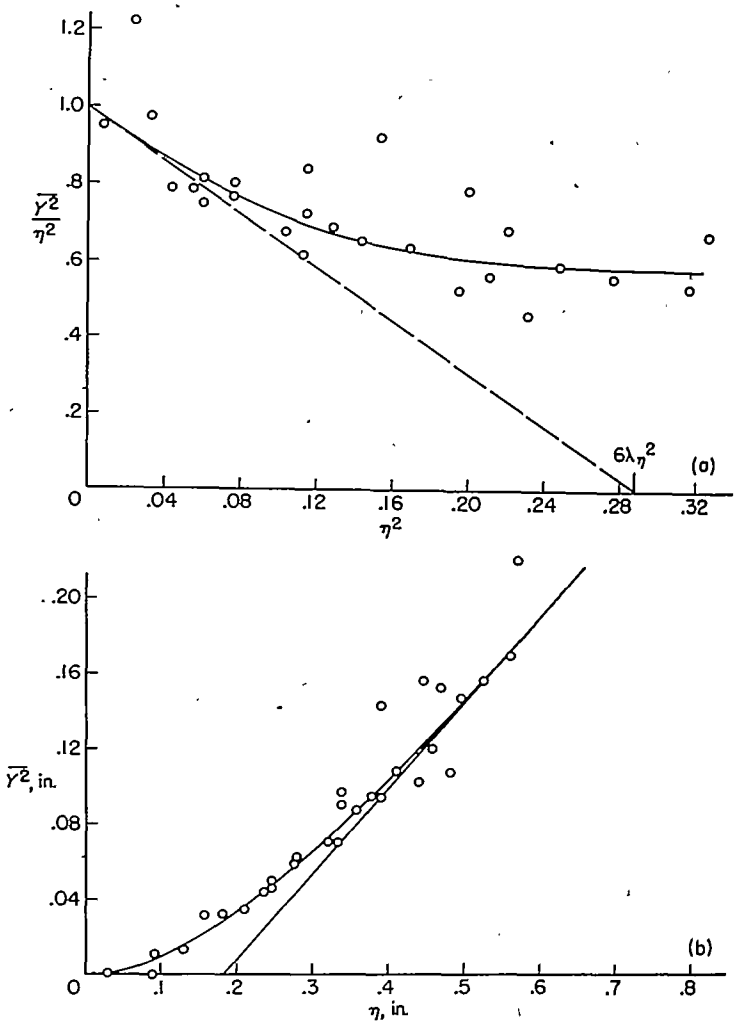

(a) $\lambda_\eta=0.22$.
(b) $L_\eta=0.23$.

FIGURE 18.—Determination of λ_η and L_η; $\frac{x_o}{M}=86.1$, $M=1$ inch, and $\overline{U}=25.6$ feet per second.

conditions can be written in the form

$$T\equiv\left(\frac{v'}{\overline{U}}\right)\left[\frac{12.5}{R_\lambda^2}+\left(\frac{\lambda}{\lambda_\eta}\right)^2\right]^{1/2}\ll 1 \tag{75}$$

From the Schwarz inequality, essentially the necessity that the magnitude of any correlation coefficient be less than or equal to unity,

$$\overline{u_i u_j\frac{\partial v}{\partial x_i}\frac{\partial v}{\partial x_j}}\leqq u_i' u_j'\left(\frac{\partial v}{\partial x_i}\right)'\left(\frac{\partial v}{\partial x_j}\right)' \tag{76}$$

where the prime in this expression denotes root-mean-square

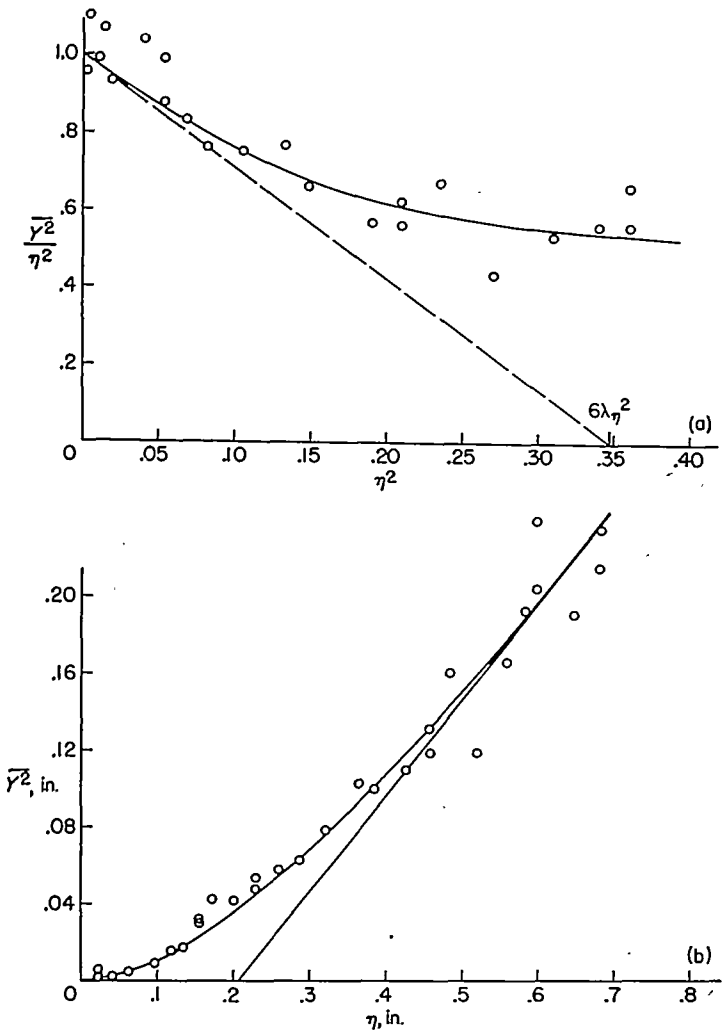

(a) $\lambda_\eta=0.24$.
(b) $L_\eta=0.25$.

FIGURE 19.—Determination of λ_η and L_η; $\frac{x_o}{M}=86.1$, $M=\frac{1}{2}$ inch, and $\overline{U}=25.6$ feet per second.

value. For isotropic turbulence, equation (76) can be written

$$\overline{u_i u_j \frac{\partial v}{\partial x_i}\frac{\partial v}{\partial x_j}} \leqq (9+4\sqrt{2})\frac{(v')^4}{\lambda^2} \tag{77}$$

Thus, the second condition in equation (26) will be satisfied if

$$2.7\frac{v'}{\overline{U}} \ll 1 \tag{78}$$

Both T and $v'/\overline{U}$ for the flows studied are presented in table I. It is clear that for these flows instantaneous x and t partial derivatives may be taken proportional with reasonable confidence.

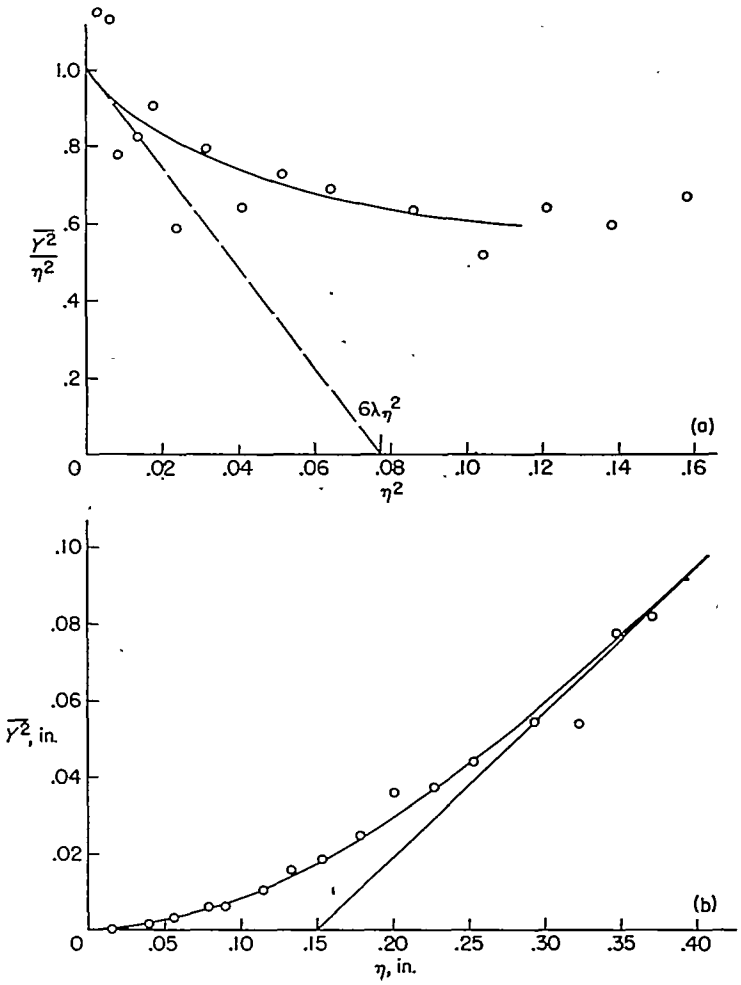

(a) $\lambda_\eta=0.11$.
(b) $L_\eta=0.19$.

FIGURE 20.—Determination of λ_η and L_η; $\frac{x_o}{M}=86.1$, $M=\frac{1}{4}$ inch, and $\overline{U}=25.6$ feet per second.

$\overline{\vartheta v}$–CORRELATION

The Eulerian measure of transverse turbulent heat transport is computed from the mean temperature distribution. The dimensionless form, $\overline{\vartheta v}/\overline{\Theta}_o\overline{U}$, is given for two typical cross sections in figures 36 and 37.

The measurements of $v'/\overline{U}$ and of $\vartheta'/\overline{\Theta}_o$ permit calculation of the correlation coefficient $R_{\vartheta v}=\frac{\overline{\vartheta v}}{\vartheta' v'}$, and this is also given in figures 36 and 37.

For the convenient and reasonably accurate assumption of Gaussian mean temperature distribution, the corresponding turbulent-heat-transfer coefficient k_T follows from equation (64). It was found to be independent of y, and typical

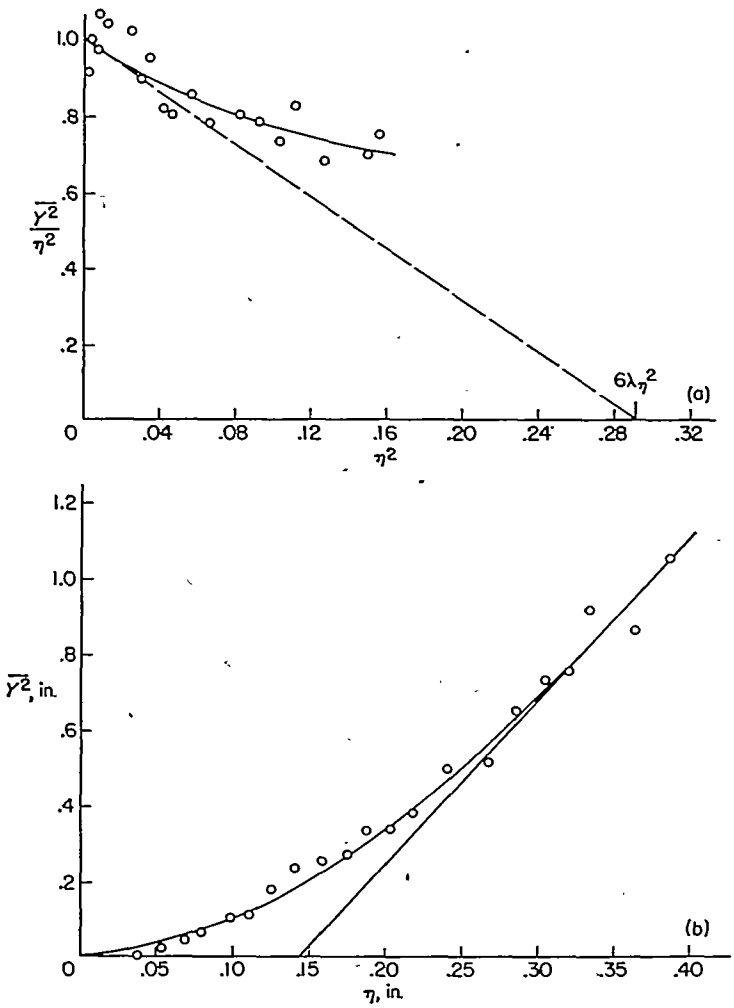

(a) λ_η=0.22.
(b) L_η=0.22.

FIGURE 21.—Determination of λ_η and L_η; $\frac{x_o}{M}$=172.3, $M=\frac{1}{2}$ inch, and $\overline{U}$=25.6 feet per second.

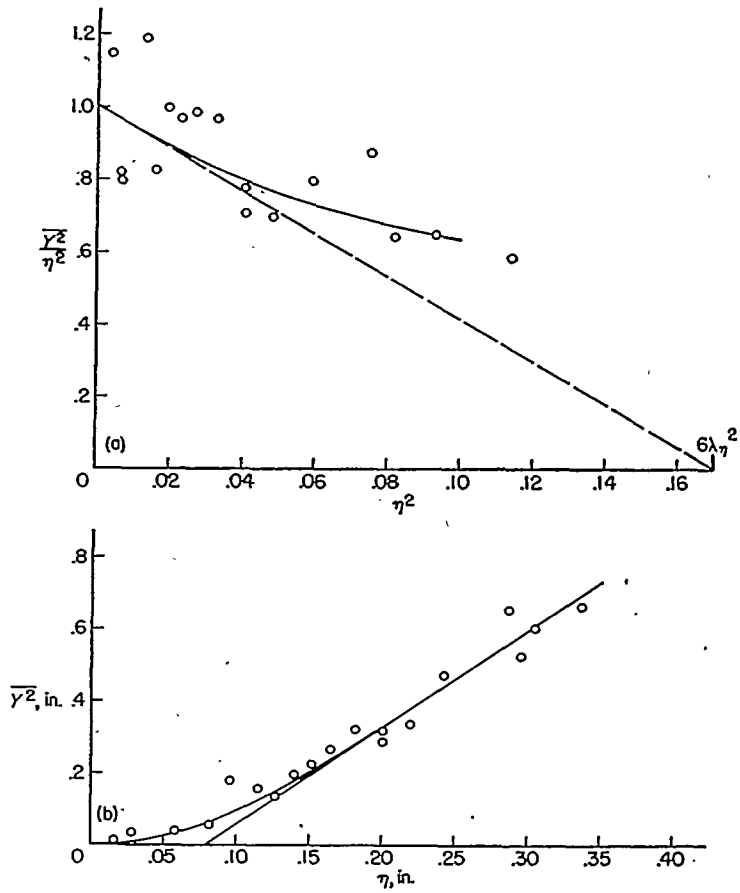

(a) λ_η=0.17.
(b) L_η=0.13.

FIGURE 22.—Determination of λ_η and L_η; $\frac{x_o}{M}$=172.3, $M=\frac{1}{4}$ inch, and $\overline{U}$=25.6 feet per second.

curves of k_T/k are given in figure 38. The data for k_T at three different speeds behind the 1-inch grid are roughly collapsed together through division of k_T by $\rho c_p v' L_\eta$, as suggested by equation (66a), an asymptotic result for nondecaying turbulence (fig. 39).

DISCUSSION

LAGRANGIAN VARIABLES

Even a cursory examination of the technique used in this investigation for the determination of Lagrangian correlation shows that, as physical measurements go, this method is a "bad" one, largely because of the inherent double differentiation between measured variable and desired information.

Figures 13 to 22 suggest an uncertainty in values of λ_η and L_η as large as ±20 percent, in spite of moderately good precision in the measurement of individual temperature distributions such as the lower curve in figure 3.

As mentioned earlier, the values of $v'/\overline{U}$ computed from initial wake spread are consistently higher than those measured with the hot-wire anemometer (reference 18). The same relative result was encountered during a brief investigation following that reported in reference 18. Up to the present time there has been no satisfactory explanation of the discrepancy. A tentative hypothesis which would at least account for its direction may be based upon a human weakness in the visual averaging of the reading of a fluctuation pointer; there seems to be a tendency to choose an

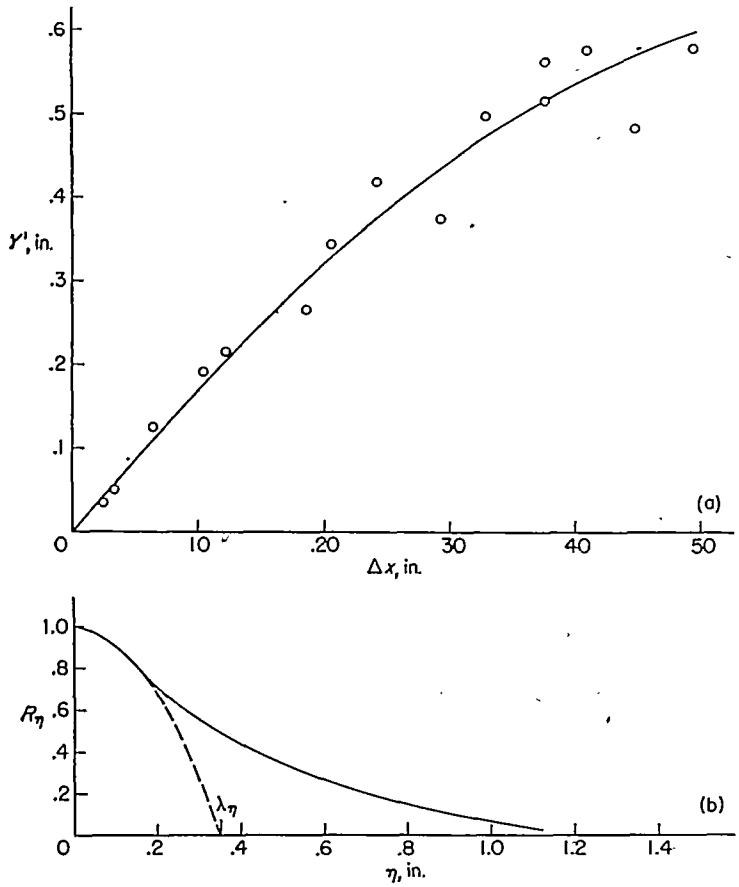

(a) Spread of heat from a line source.
(b) Correlation function R_η.

FIGURE 23.—Spread of heat from a line source and correlation function R_η for $M=1$ inch, $\bar{U}=8.5$ feet per second, and $\frac{x_o}{M}=43.4$.

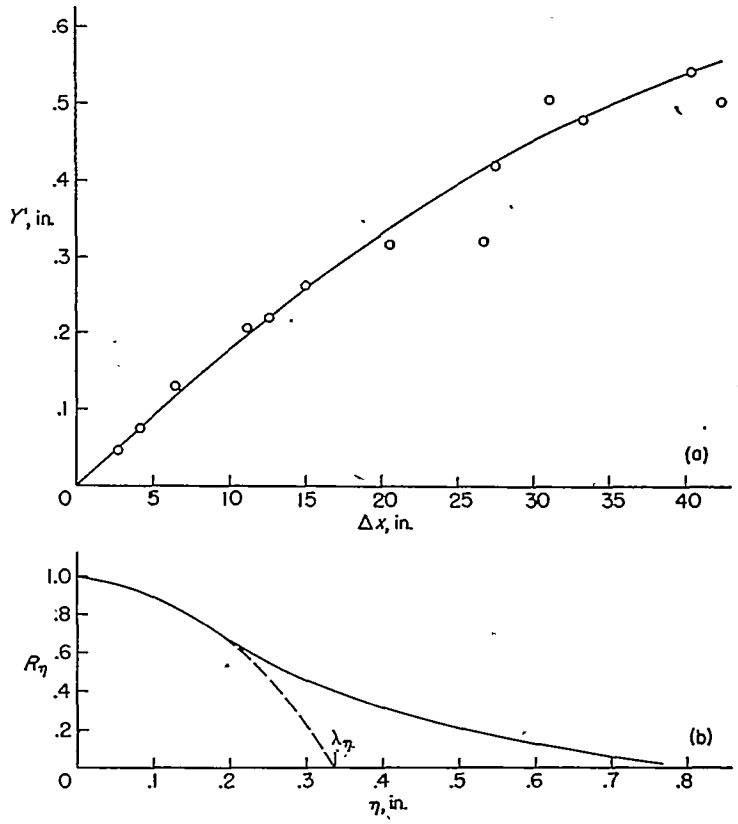

(a) Spread of heat from a line source.
(b) Correlation function R_η.

FIGURE 24.—Spread of heat from a line source and correlation function R_η for $M=1$ inch, $\bar{U}=25.6$ feet per second, and $\frac{x_o}{M}=43.4$.

"average" more or less halfway between the extremes of the needle travel. Thus a pointer motion with very skew probability density (greater than 0) would tend to be "averaged" at too high a value. The thermocouple voltage in one of these thermal wake traverses has just this character (fig. 11). Hence a visual averaging might yield too high a wake width. If this effect is nonnegligible, it is advisable to employ some electrical means of averaging for skew signals, for example, the fluxmeter and bucking circuit described in reference 10.

In view of the considerable uncertainty in λ_η as well as that in λ and v' the poor degree of agreement between experiment and theory shown in figure 33 is understandable. Since the two undetermined constants in the theoretical result have been evaluated from sets of experiments completely independent of the present ones, this agreement can be viewed as an affirmative result.

Since some sort of Lagrangian scale should be a significant length in turbulent heat and mass transport, as demonstrated in the analytical section of this report, an effort has been made to find some systematic variation in the values of L_η. Figure 34 might be construed to indicate a monotonic decrease of L_η/L with increasing values of R_L. It is interesting to note that a decrease was also observed for the ratio of mixing length to tube radius by Nikuradse (reference 30) in fully developed turbulent tube flows. In order to determine whether these two rates of decrease with increasing Reynolds numbers are of the same order of magnitude, an estimate has been made of the magnitudes of R_L corresponding to Nikuradse's results given in figures 28 and 29 of reference 30. Both scale-to-diameter ratio and average turbulent levels for various Reynolds numbers were estimated with the help of Laufer's data on turbulent channel flow (reference 31) at various Reynolds numbers. The absolute level (i. e., the ordinate scale) of the resulting l_{max}/L against R_L curve was adjusted to give the most reasonable-looking fit with the L_η/L data. This is the dashed line in

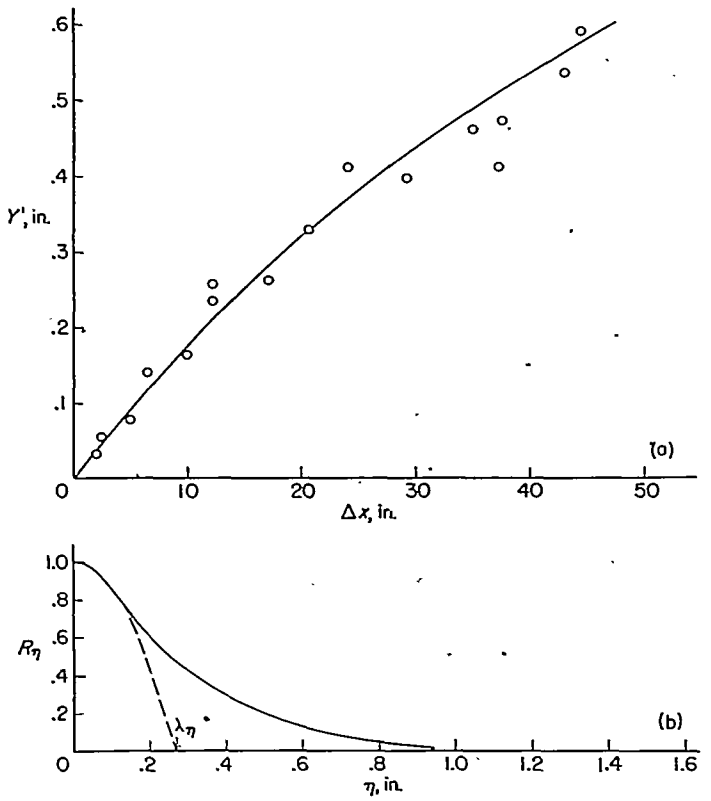

(a) Spread of heat from a line source.
(b) Correlation function R_η.

FIGURE 25.—Spread of heat from a line source and correlation function R_η for $M=1$ inch, $\overline{U}=38$ feet per second, and $\frac{x_e}{M}=43.4$.

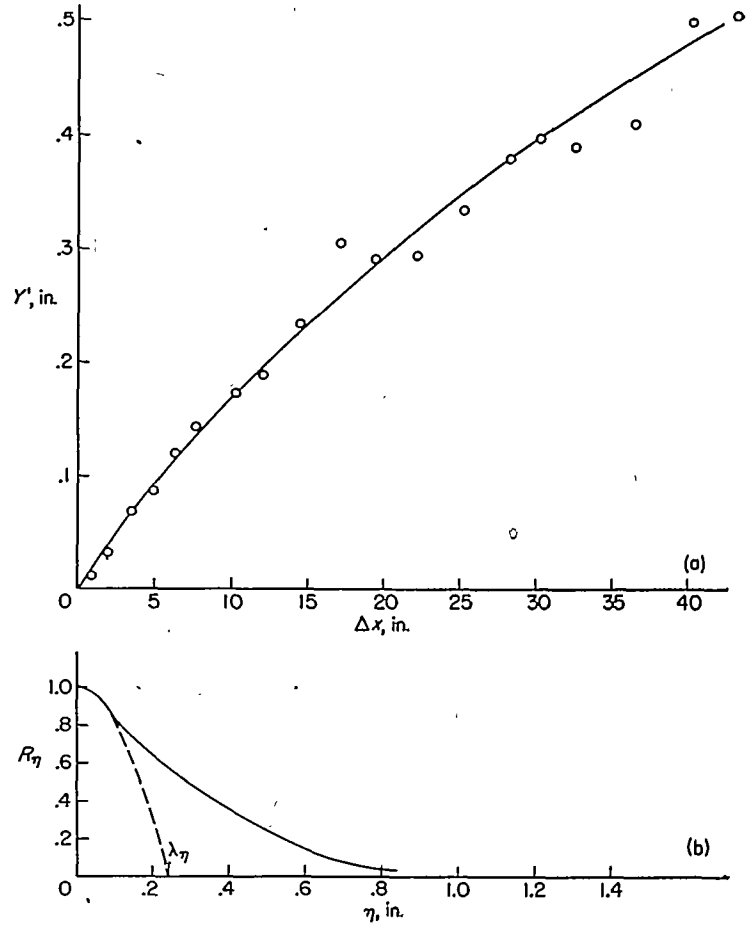

(a) Spread of heat from a line source.
(b) Correlation function R_η.

FIGURE 26.—Spread of heat from a line source and correlation function R_η for $M=\frac{1}{2}$ inch, $\overline{U}=25.6$ feet per second, and $\frac{x_e}{M}=43.4$.

figure 34 and it shows at least a qualitative resemblance. It is likely, however, that L_η/L is not a unique function of R_L.

Of course not all of the scatter in figures 34 and 35 (involving L_η) can be attributed to simple lack of experimental precision. Some is evidence of the fact that the Taylor postulate of Lagrangian correlation function being uniquely a function of η is certainly not very closely true. Furthermore, table I does show rather systematic variations of L_η in some of the three-point groups. Most noticeably, there is a regular decrease in L_η with increasing x_0/M (or perhaps with decreasing $v'/\overline{U}$) for each of the three grids.

TEMPERATURE-FLUCTUATION FIELD

Fairly close behind a line heat source in turbulent flow, the random pulse nature of the temperature fluctuations at a fixed point has been established by the oscillogram in reference 10. This is confirmed by the first two oscillograms in figure 11, with their highly skew probability densities at $\Delta x/M=10$. One of the objectives of the present investigation was to find out whether this distinctly pulsed character persisted far downstream or whether molecular heat conduction becomes increasingly effective in smearing out the pulses, until they are no longer distinguishable as such. The third oscillogram and probability density in figure 11 ($\Delta x/M=70$) does show a decided trend away from the pulse-type signal. The molecular broadening of the laminar wake (corresponding to the pulses) decreases the relative spacing of the pulses in $\vartheta(t)$ at any point in the "turbulent wake" region. This is a reduction in relative length of the flat ($\vartheta=0$) base lines between pulses, giving greater statistical symmetry in $\vartheta(t)$ about its mean, that is, reducing the skewness of $P(\vartheta)$.

A simple analysis will show the existence of an asymptotic

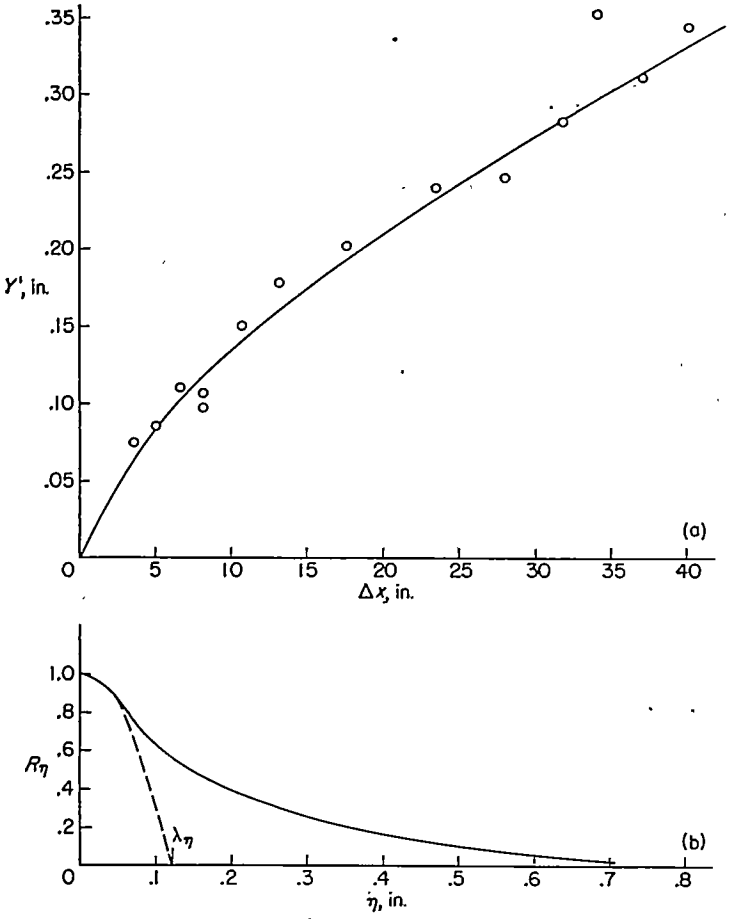

(a) Spread of heat from a line source.
(b) Correlation function R_η.

FIGURE 27.—Spread of heat from a line source and correlation function R_η for $M=\frac{1}{4}$ inch, $\overline{U}=25.6$ feet per second, and $\frac{x_o}{M}=43.4$.

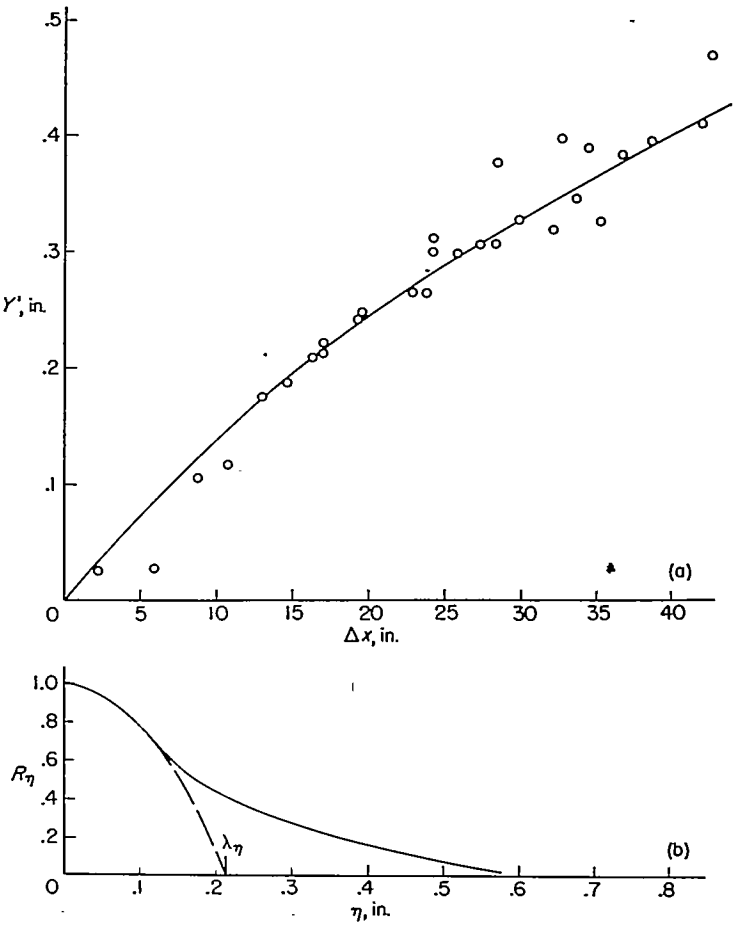

(a) Spread of heat from a line source.
(b) Correlation function R_η.

FIGURE 28.—Spread of heat from a line source and correlation function R_η for $M=1$ inch, $\overline{U}=25.6$ feet per second, and $\frac{x_o}{M}=86.1$.

behavior of molecular-conduction effects in a nondecaying turbulence. For a nondecaying flow turbulence and very large values of $t(\approx x/\overline{U})$ the mean-square wake spread due to turbulent motion is

$$\overline{Y^2}\approx 2L_\eta\frac{v'}{\overline{U}}x \tag{79}$$

On the other hand, an approach to molecular diffusion through Taylor's concept of "continuous movements" gives, for any macroscopic distance downstream, the mean-square thermal wake width,

$$\overline{Y_m^2}\approx 2\Lambda\frac{c}{\overline{U}}x \tag{80}$$

where Λ is the mean free path and c is the root-mean-square molecular velocity.

From equations (79) and (80)

$$\frac{Y_m'}{Y'}\approx\left(\frac{\Lambda}{L_\eta}\frac{c}{v'}\right)^{1/2} \tag{81}$$

For a typical case, take $L=1$ centimeter, $v'=10$ centimeters per second, $\Lambda=6\times10^{-6}$ centimeter, and $c=5\times10^4$ centimeters per second. Then $\frac{Y_m'}{Y'}\approx0.17$. For people accustomed to thinking of molecular transport as negligibly small in turbulent flow (e. g., in shear flow), this ratio will appear quite large. The values of k_T/k plotted in figure 38 also show that at these low turbulence levels the molecular thermal conductivity is not necessarily negligible compared with the turbulent transport.

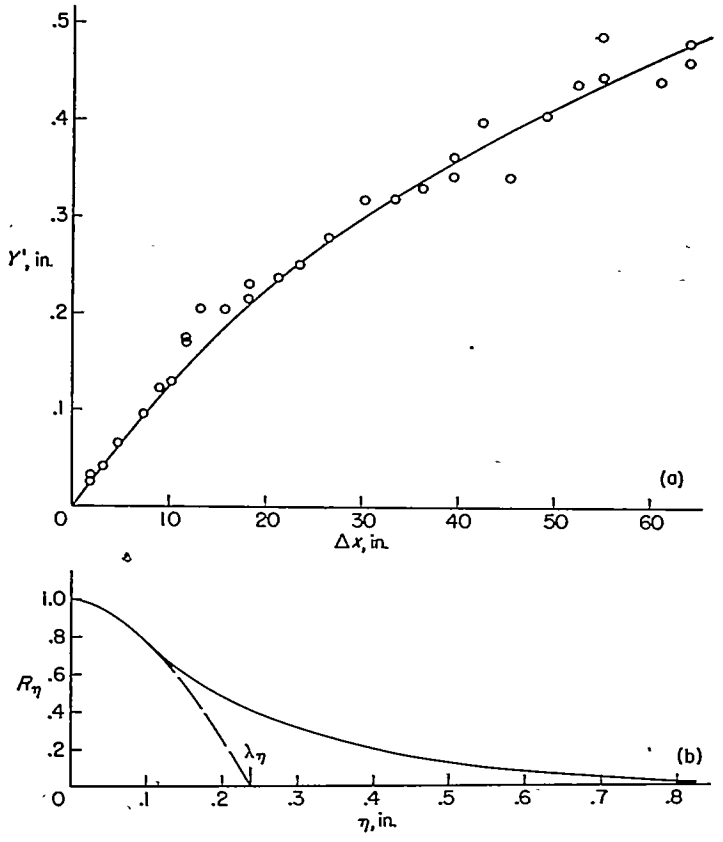

(a) Spread of heat from a line source.
(b) Correlation function R_η.

FIGURE 29.—Spread of heat from a line source and correlation function R_η for $M=\frac{1}{2}$ inch, $\overline{U}=25.6$ feet per second, and $\frac{x_o}{M}=86.1$.

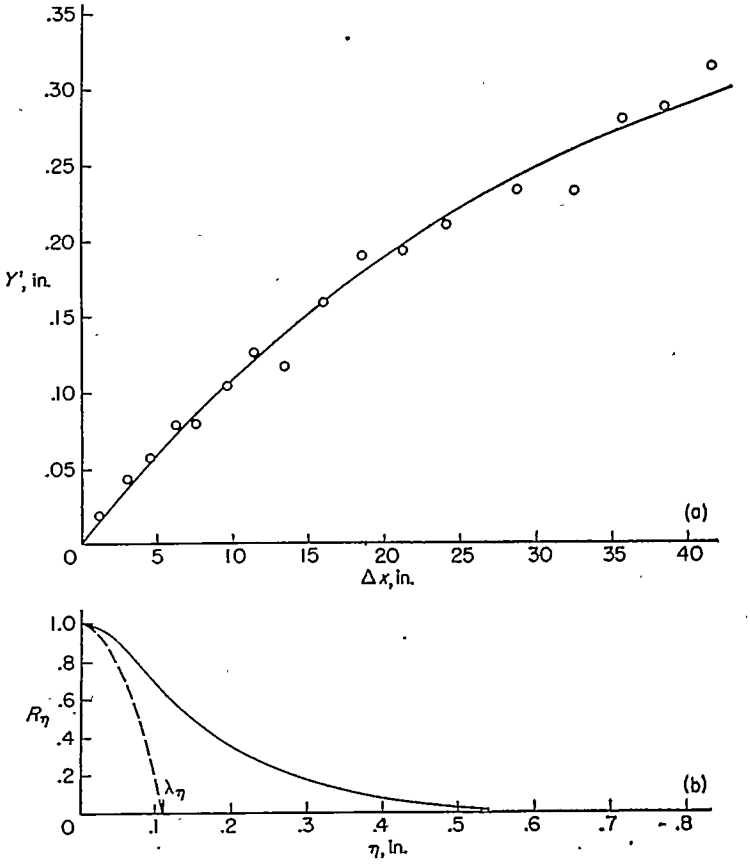

(a) Spread of heat from a line source.
(b) Correlation function R_η.

FIGURE 30.—Spread of heat from a line source and correlation function R_η for $M=\frac{1}{4}$ inch, $\overline{U}=25.6$ feet per second, and $\frac{x_o}{M}=86.1$.

The temperature-fluctuation-level distributions $\vartheta'/\overline{\Theta}$ across the wake (figs. 10 (a) and 10 (b)) show the same character as that measured at much higher turbulence level in a jet (reference 10), with somewhat lower minimum values, which are attributable to the lower turbulence level. A rough evaluation of the behavior of the statistical variables in this turbulent thermal wake is obtainable by recalling that it consists of a randomly "waving" laminar thermal wake. If $\vartheta(t)$ is crudely represented by a randomly spaced sequence of identical rectangular pulses with height ϑ_o, width j, and average spacing s, it is easily seen that

$$\overline{\Theta}=\frac{\vartheta_o j}{s} \tag{82}$$

$$\frac{\vartheta'}{\overline{\Theta}}=\left(\frac{s}{j}-1\right)^{1/2} \tag{83}$$

This permits $\vartheta'/\overline{\Theta}$ to vary between 0 and ∞ as s/j travels the permissible range from 1 to ∞. Since points nearer the edge of the turbulent thermal wake have higher values of s/j, the behavior of equation (83) is consistent with the experimental distribution. If the analysis were repeated with triangular pulses, for example, the quantitative estimate would doubtless be more realistic. The higher values of $(\vartheta'/\overline{\Theta})_{min}$ encountered at higher values of $v'/\overline{U}$ are an indication that for a given width of laminar thermal wake, the higher value of $v'/\overline{U}$ leads to a higher minimum value of s/j.

The closely Gaussian shape of $\overline{\Theta}/\overline{\Theta}_o$ against y has already been pointed out. If

$$\frac{\overline{\Theta}}{\overline{\Theta}_o}=\exp\left[-\frac{1}{2}\frac{y^2}{(Y')^2}\right]$$

be introduced, there results

$$\frac{\vartheta'}{\overline{\Theta}}=\left\{\frac{\vartheta_o}{\overline{\Theta}_o}\exp\left[\frac{1}{2}\frac{y^2}{(Y')^2}\right]-1\right\}^{1/2} \tag{84}$$

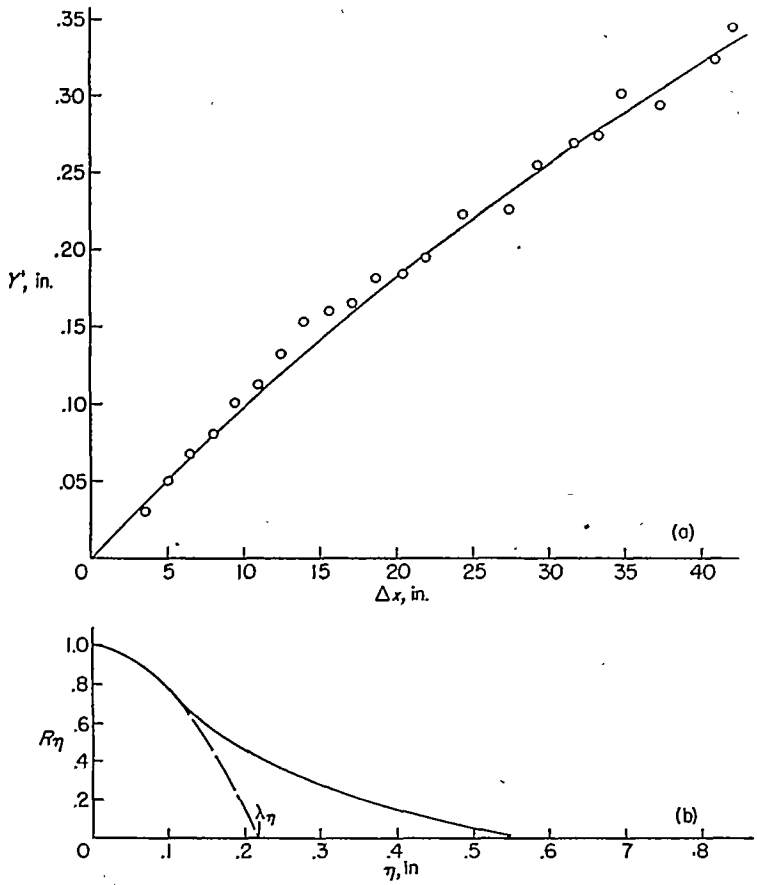

(a) Spread of heat from a line source.
(b) Correlation function R_η.

FIGURE 31.—Spread of heat from a line source and correlation function R_η for $M=\frac{1}{2}$ inch, $\overline{U}=25.6$ feet per second, and $\frac{x_o}{M}=172.3$.

and

$$\frac{\vartheta'}{\overline{\Theta}_o}=\exp\left[-\frac{1}{2}\frac{y^2}{(Y')^2}\right]\left\{\frac{\vartheta_o}{\overline{\Theta}}\exp\left[\frac{1}{2}\frac{y^2}{(Y')^2}\right]-1\right\}^{1/2} \tag{85}$$

Both of these expressions have behavior consistent with the experiments.

The form of dimensionless transverse turbulent-heat-transfer rate $\overline{\vartheta v}/\overline{\Theta}_o\overline{U}$ can be deduced for small values of Δx (such that $R_\eta \approx 1$) with this pulse representation of $\vartheta(t)$. In this picture, $\overline{\vartheta v}$ is the correlation between a continuous random variable v and a random pulse signal ϑ which "fires" every time the continuous variable passes through a specific value

$$v_1=\frac{y}{\Delta x}\overline{U}$$

Therefore

$$\overline{\vartheta v}=\frac{\vartheta_o j}{s}\frac{y}{\Delta x}\overline{U}$$

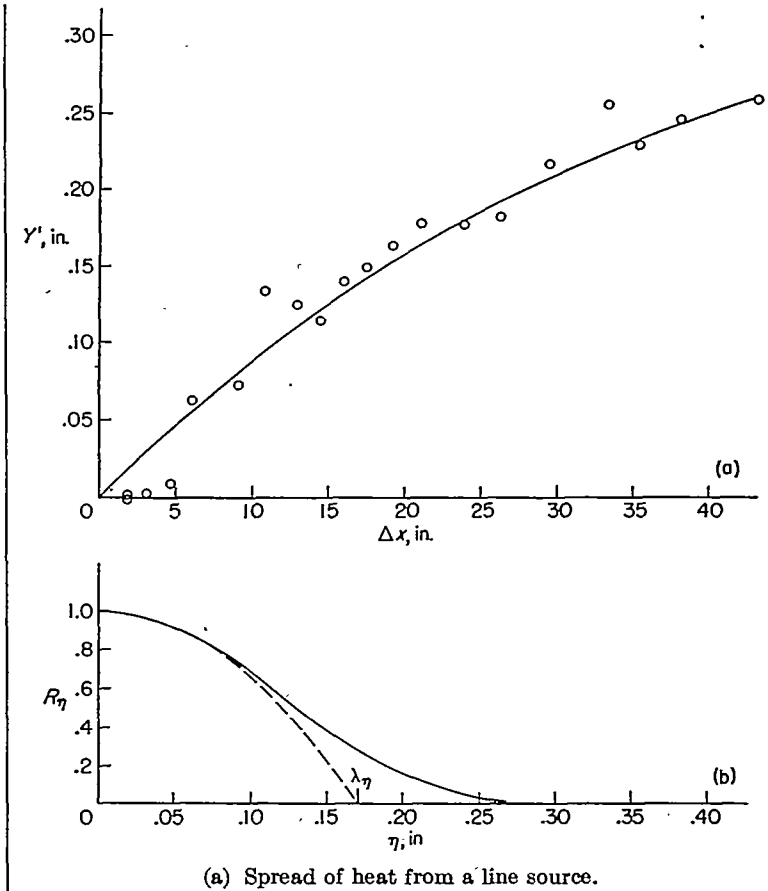

(a) Spread of heat from a line source.
(b) Correlation function R_η.

FIGURE 32.—Spread of heat from a line source and correlation function R_η for $M=\frac{1}{4}$ inch, $\overline{U}=25.6$ feet per second, and $\frac{x_o}{M}=172.3$.

$$\overline{\vartheta v}=\frac{\overline{U}}{\Delta x}\bar{\Theta}y \tag{86}$$

where s and $\bar{\Theta}$ are functions of y. With Gaussian $\bar{\Theta}(y)$,

$$\frac{\overline{\vartheta v}}{\overline{\Theta}_o\overline{U}}=\frac{y}{\Delta x}\exp\left[-\frac{1}{2}\frac{y^2}{(Y')^2}\right] \tag{87}$$

The direct comparison between this crude picture and the experimental results will be confined to the correlation coefficient $R_{\vartheta v}=\overline{\vartheta v}/\vartheta' v'$. This is of particular interest in view of the surprisingly high experimental values. With equation (85) and the fact that $v'/\overline{U}=Y'/\Delta x$, there results

$$R_{\vartheta v}=\frac{y}{Y'}\left\{\frac{\vartheta_o}{\overline{\Theta}_o}\exp\left[\frac{1}{2}\frac{y^2}{(Y')^2}\right]-1\right\}^{-1/2} \tag{88}$$

This contains the undetermined constant $\vartheta_o/\overline{\Theta}_o$, which can be obtained from any one of several experimental results. Figure 36 includes one plot of equation (88) with $\vartheta_o/\overline{\Theta}_o$ de-

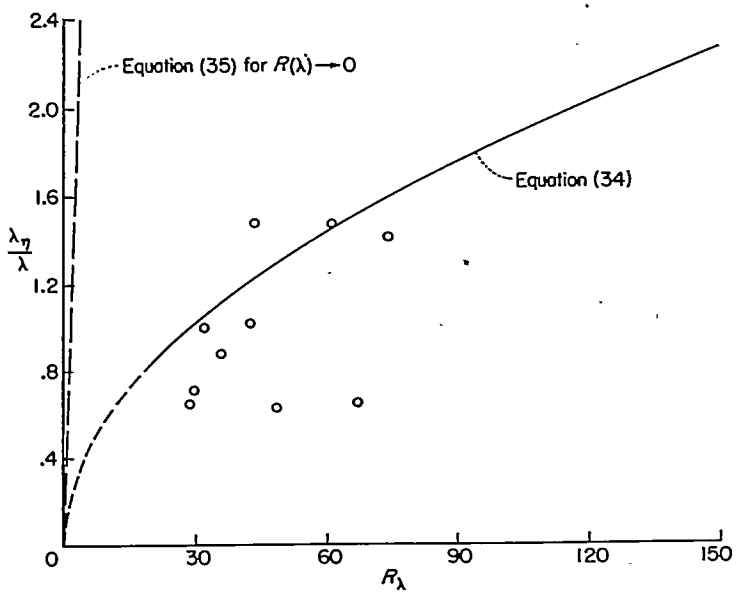

FIGURE 33.—Ratio of Lagrangian and Eulerian microscales.

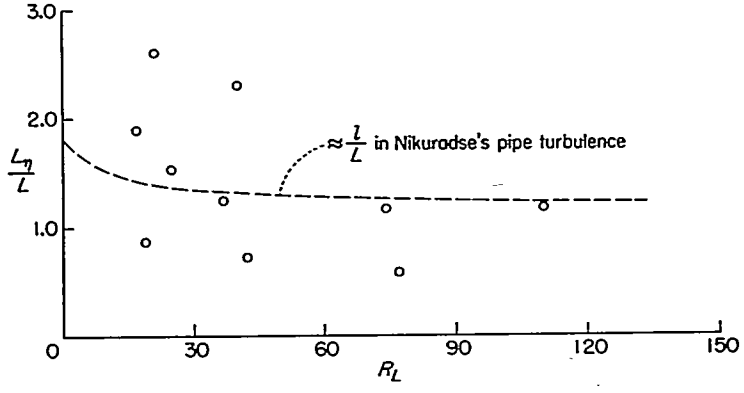

FIGURE 34.—Ratio of Lagrangian and Eulerian scales.

termined from equation (84) and the experimental value of $(\vartheta'/\overline{\Theta})_{min}$ and one plot with $\vartheta_o/\overline{\Theta}$ determined by matching equation (88) with the experimental result at $y/Y'=1.4$.

It is also surprising to find that the experimental $(R_{\vartheta v})_{max}$ at large values of Δx is even larger than that at small values of Δx. This may be due to a considerable experimental error; the resistance-thermometer voltage signal is much lower here. Unfortunately no relation corresponding to equation (88) has been deduced for large values of Δx, where R_η is essentially zero.

The criteria for Taylor's hypothesis of the interchangeability of instantaneous space $\overline{U}\frac{\partial}{\partial x}$ and time $\frac{\partial}{\partial t}$ derivatives (assumed by him to depend only upon turbulence level) have been expressed in equations (75) and (78) as functions of turbulence level R_λ and λ/λ_η. If λ/λ_η is replaced by its theoretical expression (equation (34)) in terms of R_η, equation (75) becomes

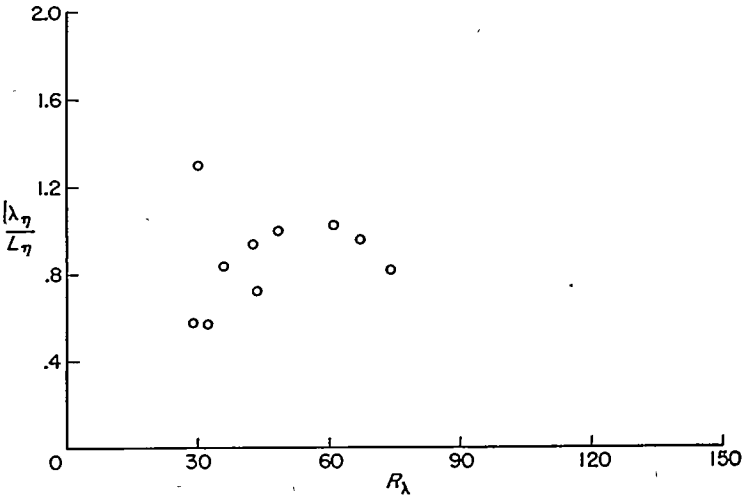

FIGURE 35.—Ratio of Lagrangian microscale and scale.

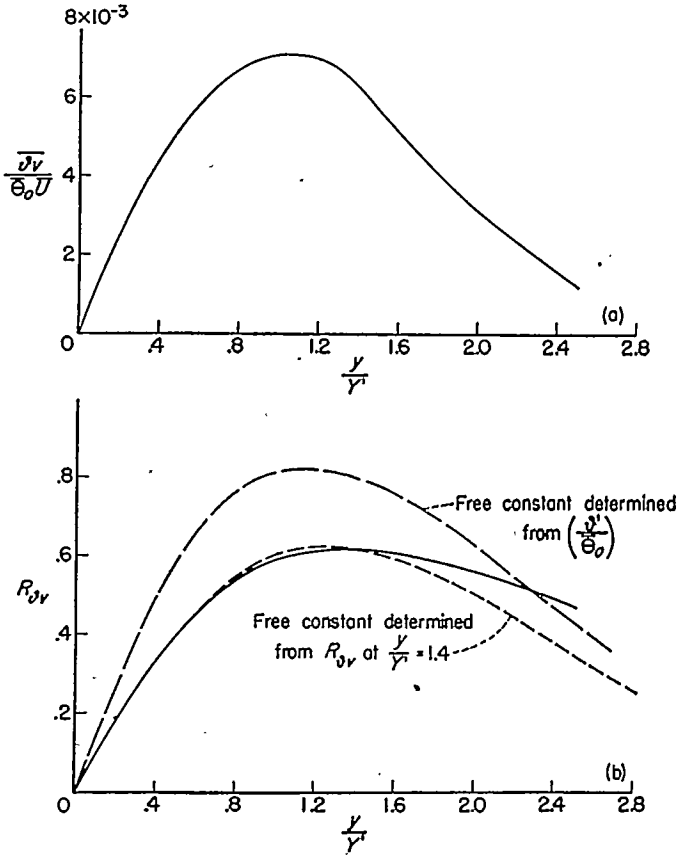

(a) $\frac{\overline{\vartheta v}}{\Theta_o \overline{U}}$ against $\frac{y}{Y'}$

(b) $R_{\vartheta v}$ against y/Y'. Dashed curves are result of analysis based on rectangular temperature pulses.

FIGURE 36.—Heat-transfer correlation across thermal wake, computed from measured mean temperature distribution. $\overline{U}=25.6$ feet per second, $M=1$ inch, $x_o=43.4$ inches, and $\Delta x=10.5$ inches.

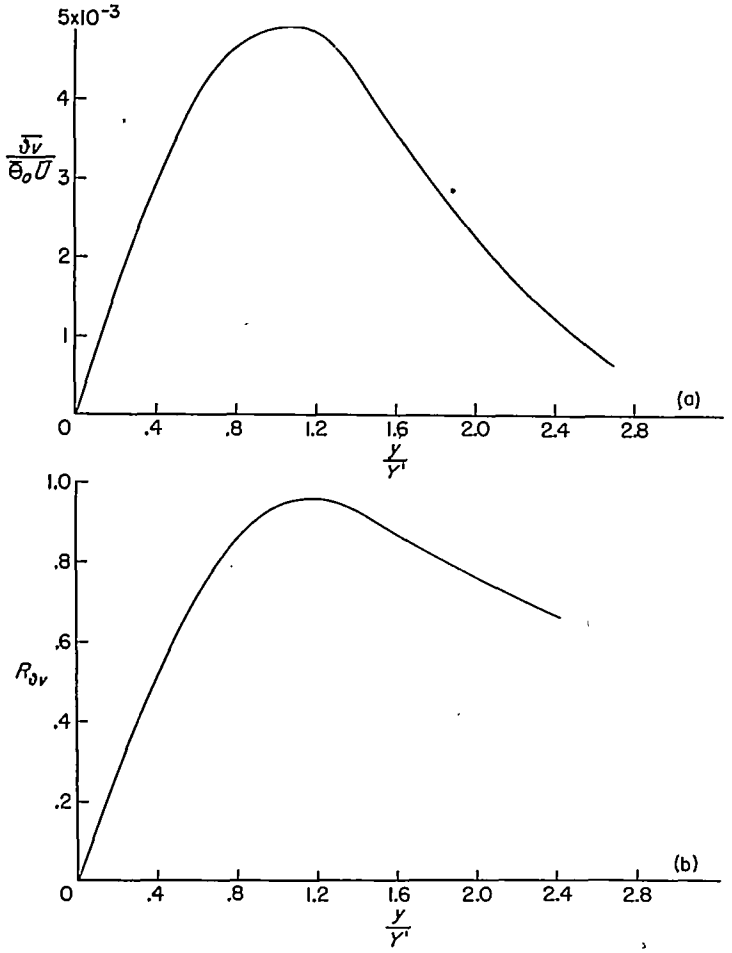

(a) $\frac{\overline{\partial v}}{\theta_o \overline{U}}$ against $\frac{y}{Y'}$.

(b) $R_{\partial v}$ against y/Y'.

FIGURE 37.—Heat-transfer correlation across thermal wake, computed from measured mean temperature distribution. $\overline{U}$=25.6 feet per second, M=1 inch, x_o=43.4 inches, and Δx=70 inches.

$$\frac{v'}{\overline{U}}\left(\frac{25}{R_\lambda^2}+\frac{29}{R_\lambda}\right)^{1/2} \ll 1 \tag{89}$$

For estimates of most flows the first term in the parentheses can be neglected; values of R_λ less than 5 or 10 are rare.

Since equation (34) has now been roughly verified by experiment, equations (89) and (78) may serve as approximate criteria for the validity of Taylor's hypothesis.

In the limit of $R_\lambda \to 0$ when equation (35) replaces equation (34), there follows a simpler criterion to replace equation (75):

$$\frac{4}{R_\lambda}\left(\frac{v'}{\overline{U}}\right) \ll 1 \tag{90}$$

SUMMARY OF RESULTS

The following results were obtained from the investigation of the diffusion of heat from a line source in isotropic turbulence.

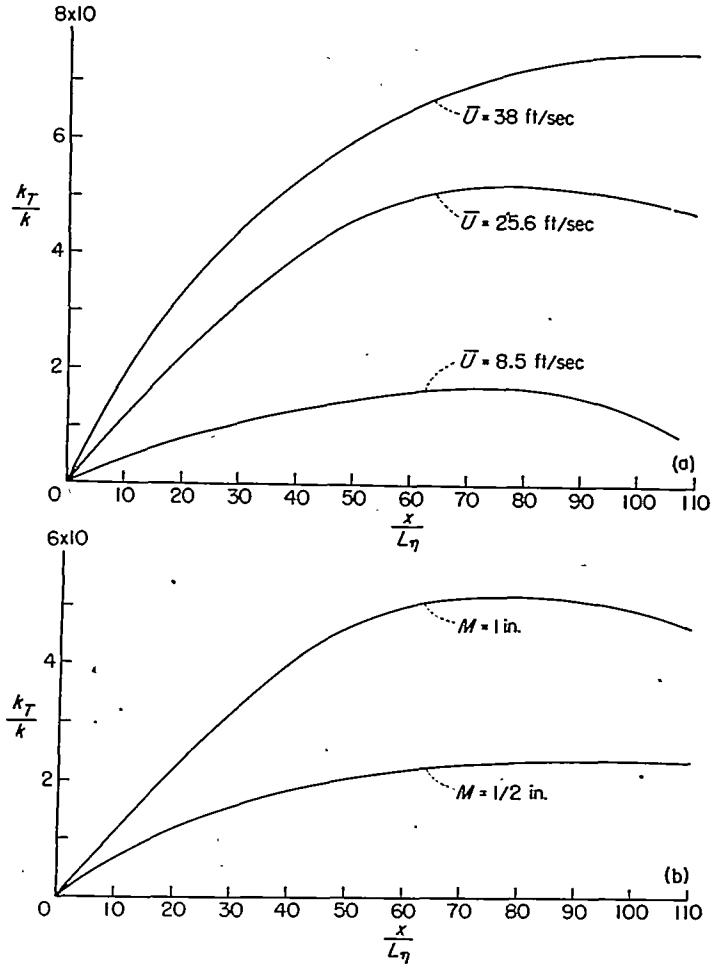

(a) Turbulent-heat-transfer coefficient at three airspeeds. M=1 inch and $\frac{x_o}{M}$=43.4.

(b) Turbulent-heat-transfer coefficient for two different grids. $\overline{U}$=25.6 feet per second and $\frac{x_o}{M}$=43.4.

FIGURE 38.—Turbulent-heat-transfer coefficient for three airspeeds and two different grids.

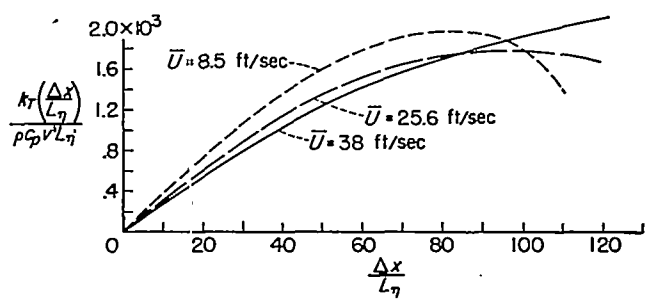

FIGURE 39.—Dimensionless turbulent-heat-transfer coefficient. $\frac{x_o}{M}$=43.4 and M=1 inch.

1. The thermal wake behind a heated wire set perpendicular to a flowing isotropic turbulence (at sufficiently low wire Reynolds number) consists of a randomly "waving" thin, laminar, thermal wake whose variations in lateral position give what may be called the turbulent thermal wake. At a fixed point not too far behind the wire the instantaneous temperature difference $\vartheta(t)$ is a random pulse function, and the nature of the turbulent heat transfer can be deduced on this basis. Farther downstream the distinct pulse nature tends to disappear.

2. The mean transverse temperature distribution $\frac{\overline{\theta}}{\overline{\theta}_o}(y)$ appears to be Gaussian within the experimental precision for all distances behind the wire.

3. An Eulerian analysis of this turbulent-heat-transfer problem permits computation of the turbulent-heat-transfer coefficient k_T which is essentially constant with respect to the distance in the direction of the measured diffusion y for these boundary conditions. It is found that at low turbulence levels (approximately equal to 1 to 2 percent) the molecular heat transport is not vanishingly small compared with the turbulent heat transport.

4. Although Taylor's postulate that Lagrangian correlations in decaying turbulence can be made similar by introduction of an independent variable $\eta=\int_0^t v'(t)dt$ (where t is time and v' is the root-mean-square instantaneous velocity fluctuation in the y-direction) seems to be an oversimplification, it has been applied here for convenience in the reduction of data. A simple comparison of Eulerian and Lagrangian analyses for diffusion in nondecaying turbulence shows that for large values of the distance from the heat source Δx the Lagrangian scale L_η enters the expression for k_T, the turbulent-heat-transfer coefficient, much like the empirical mixing length in the old turbulent transport theories. Therefore some properly modified generalization of Taylor's η-postulate should prove useful.

5. A correction and generalization of Heisenberg's theoretical expression for the ratio of Eulerian to Lagrangian microscale λ/λ_η as a function only of the turbulence Reynolds number based on microscale R_λ has been made and seems to agree roughly with experiment. It must be noted that since λ_η depends only upon a transformation $d\eta=v'dt$, and not upon the integral postulate stated above, its validity is not impaired by any failure of the integral postulate

6. Taylor's hypothesis for the interchangeability of space and time derivatives at low turbulence levels has been expressed in terms of criteria which depend upon turbulence level, Reynolds number, and λ/λ_η. Applied to the flows studied here it shows that in these cases such a transformation is permissible. By substitution of the theoretical expression for $\frac{\lambda}{\lambda_\eta}(R_\lambda)$, a slightly simpler and rougher criterion is derived, depending only upon turbulence level and R_λ.

THE JOHNS HOPKINS UNIVERSITY,
BALTIMORE, MD., *June 5, 1951.*

REFERENCES

1. Taylor, G. I.: Diffusion by Continuous Movements. Proc. London Math. Soc., ser. A, vol. 20, 1921, pp. 196–212.
2. Taylor, G. I.: Statistical Theory of Turbulence. Parts I–IV. Proc. Roy. Soc. (London), ser. A, vol. 151, no. 873, Sept. 2, 1935, pp. 421–478.
3. Batchelor, G. K.: Diffusion in a Field of Homogeneous Turbulence. Australian Jour. Sci. Res., ser. A, vol. 2, no. 4, Dec. 1949, pp. 437–450.
4. Schubauer, G. B.: A Turbulence Indicator Utilizing the Diffusion of Heat. NACA Rep. 524, 1935.
5. Kampé de Feriet, J. M.: Les fonctions aleatoires stationnaires et la theorie statistique de la turbulence homogene. Ann. Soc. Sci. (Bruxelles), vol. 59, ser. 1, 1939, pp. 145–194.
6. Frenkiel, F. N.: On Turbulent Diffusion. Rep. 1136, Symposium on Turbulence (June 1949), Naval Ord. Lab., July 1, 1950, pp. 67–86.
7. Collis, D. C.: The Diffusion Process in Turbulent Flow. Rep. A.55, Div. Aero., Australian Council Sci. and Ind. Res., Dec. 1948.
8. Skramstad, H. K., and Schubauer, G. B.: The Application of Thermal Diffusion to the Study of Turbulent Air Flow. Phys. Rev., vol. 53, no. 11, June 1, 1938, p. 927.
9. Dryden, Hugh L.: Turbulence and Diffusion. Ind. and Eng. Chem., vol. 31, no. 4, April 1939, pp. 416–425.
10. Corrsin, Stanley, and Uberoi, Mahinder S.: Spectra and Diffusion in a Round Turbulent Jet. NACA Rep. 1040, 1951. (Supersedes NACA TN 2124.)
11. Kalinske, A. A., and Pien, C. L.: Eddy Diffusion. Ind. and Eng. Chem., vol. 36, no. 3, March 1944, pp. 220–223.
12. Van Driest, E. R.: Experimental Investigation of Turbulence Diffusion—A Factor in Transportation of Sediment in Open-Channel Flow. Jour. Appl. Mech., vol. 12, no. 2, June 1945, pp. A–91—A–100.
13. Simmons, L. F. G., and Salter, C.: Experimental Investigation and Analysis of the Velocity Variations in Turbulent Flow. Proc. Roy. Soc. (London), ser. A, vol. 145, no. 854, June 1934, pp. 212–234.
14. Dryden, Hugh L., Schubauer, G. B., Mock, W. C., Jr., and Skramstad, H. K.: Measurements of Intensity and Scale of Wind-Tunnel Turbulence and Their Relation to the Critical Reynolds Number of Spheres. NACA Rep. 581, 1937.
15. Hall, A. A.: Measurements of the Intensity and Scale of Turbulence. R. & M. No. 1842, British A. R. C., 1938.
16. Von Kármán, Th.: Some Remarks on the Statistical Theory of Turbulence. Proc. Fifth Int. Cong. Appl. Mech. (Sept. 1938, Cambridge, Mass.), John Wiley & Sons, Inc., 1939, pp. 347–351.
17. Dryden, Hugh L.: A Review of the Statistical Theory of Turbulence. Quart. Appl. Math., vol. I, no. 1, April 1943, pp. 7–42.
18. Corrsin, S.: Decay of Turbulence Behind Three Similar Grids. A. E. Thesis, C. I. T., 1942.
19. Batchelor, G. K., and Townsend, A. A.: Decay of Vorticity in Isotropic Turbulence. Proc. Roy. Soc. (London), ser. A., vol. 190, no. 1023, Sept. 9, 1947, pp. 534–550.
20. Batchelor, G. K., and Townsend, A. A.: Decay of Isotropic Turbulence in the Initial Period. Proc. Roy. Soc. (London), ser. A, vol. 193, no. 1035, July 21, 1948, pp. 539–558.
21. Corrsin, Stanley: Extended Applications of the Hot-Wire Anemometer. NACA TN 1864, 1949; abstract in Rev. Sci. Instr., vol. 18, no. 7, July 1947, pp. 469–471.
22. Batchelor, G. K.: Pressure Fluctuations in Isotropic Turbulence. Proc. Cambridge Phil. Soc., vol. 47, pt. 2, July 1951, pp. 359–374.
23. Taylor, G. I.: The Spectrum of Turbulence. Proc. Roy. Soc. (London), ser. A, vol. 164, no. 919, Feb. 18, 1938, pp. 476–490.
24. Lin, C. C.: On Taylor's Hypothesis in Wind-Tunnel Turbulence. Memo. No. 10775, Naval Ord. Lab., Feb. 20, 1950.
25. Heisenberg, W.: Zur statistischen Theorie der Turbulenz. Zeitschr. Phys., Bd. 124, Heft 7/12, 1948, pp. 628–657.

26. Chandrasekhar, S.: On Heisenberg's Elementary Theory of Turbulence. Proc. Roy. Soc. (London), ser. A, vol. 200, no. 1060, Dec. 1949, pp. 20–33.

27. De Kármán, Theodore, and Howarth, Leslie: On the Statistical Theory of Isotropic Turbulence. Proc. Roy. Soc. (London), ser. A, vol. 164, no. 917, Jan. 1938, pp. 192–215.

28. Lee, T. D.: Note on the Coefficient of Eddy Viscosity in Isotropic Turbulence. Phys. Rev., vol. 77, no. 6, March 15, 1950, pp. 842–843.

29. Proudman, I.: A Comparison of Heisenberg's Spectrum of Turbulence With Experiment. Proc. Cambridge Phil. Soc., vol. 47, pt. 1, Jan. 1951, pp. 158–176.

30: Nikuradse, J.: Regularity of Turbulent Flow in Smooth Tubes. Tech. Memo. No. Pur–11, Project Squid, Polytechnic Inst. of Brooklyn, Aug. 1949. (Trans. from: Forsch. 356, supp. to Forsch. Geb. Ing.-Wes., Bd. 3, Heft 2, Sept.–Oct. 1932.)

31. Laufer, John: Investigation of Turbulent Flow in a Two-Dimensional Channel. NACA Rep. 1053, 1951. (Supersedes NACA TN 2123.)

TABLE I

RESULTS FOR LAGRANGIAN AND EULERIAN SCALES AND MICROSCALES

$\overline{U}$ (fps)	M (in.)	x_0/M	$v'/\overline{U}$ (percent)	λ (in.)	λ_g (in.)	L (in.)	L_g (in.)	λ_g/λ	L_g/L	R_λ	R_L	T
8.5	1	43.4	2.0	0.41	0.36	0.28	0.43	0.88	1.54	36	25	0.0228
25.6	1	43.4	2.0	.23	.34	.28	.33	1.48	1.18	61	74	.0136
38.0	1	43.4	2.0	.19	.27	.28	.33	1.42	1.18	74	110	.0150
25.6	1	43.4	2.0	0.23	0.34	0.28	0.33	1.48	1.18	61	74	0.0136
	½	43.4	2.0	.165	.245	.15	.34	1.48	2.3	43.5	40	.0136
	¼	43.4	2.0	.12	.12	.08	.21	1.00	2.6	32	21	.0202
25.6	1	86.1	1.5	0.34	0.22	0.39	0.23	0.65	0.59	67	77	0.0225
	½	86.1	1.4	.23	.235	.20	.25	1.02	1.25	42.5	37	.0133
	¼	86.1	1.3	.17	.11	.10	.19	.65	1.9	29	17	.0203
25.6	½	43.4	2.0	0.165	0.245	0.15	0.34	1.48	2.3	43.5	40	0.0136
		86.1	1.4	.23	.235	.20	.25	1.02	1.25	42.5	37	.0133
		172.3	1.05	.35	.22	.30	.22	.63	.73	49	42	.0164
25.6	¼	43.4	2.0	0.12	0.12	0.08	0.21	1.00	2.6	32	21	0.0202
		86.1	1.3	.17	.11	.10	.19	.65	1.9	29	17	.0203
		172.3	.95	.24	.17	.15	.13	.71	.87	30	19	.0137